Direct Forcing of Regional Currents by Sea Ice.

Stefan Jendersie[1;2],
Pat Langhorne[1], Michael J. M. Williams[2], Robin Robertson[3]

[1]University of Otago, Department of Physics, Dunedin, New Zealand
[2]National Institute of Water and Atmospheric Research (NIWA), Wellington, New Zealand
[3]UNSW@ADFA, School of Physical, Environmental and Mathematical Sciences, Canberra, Australia

ROMS Asia Pacific Workshop
Hobart, October 17 – 20, 2016

Ross Sea

Antarctica

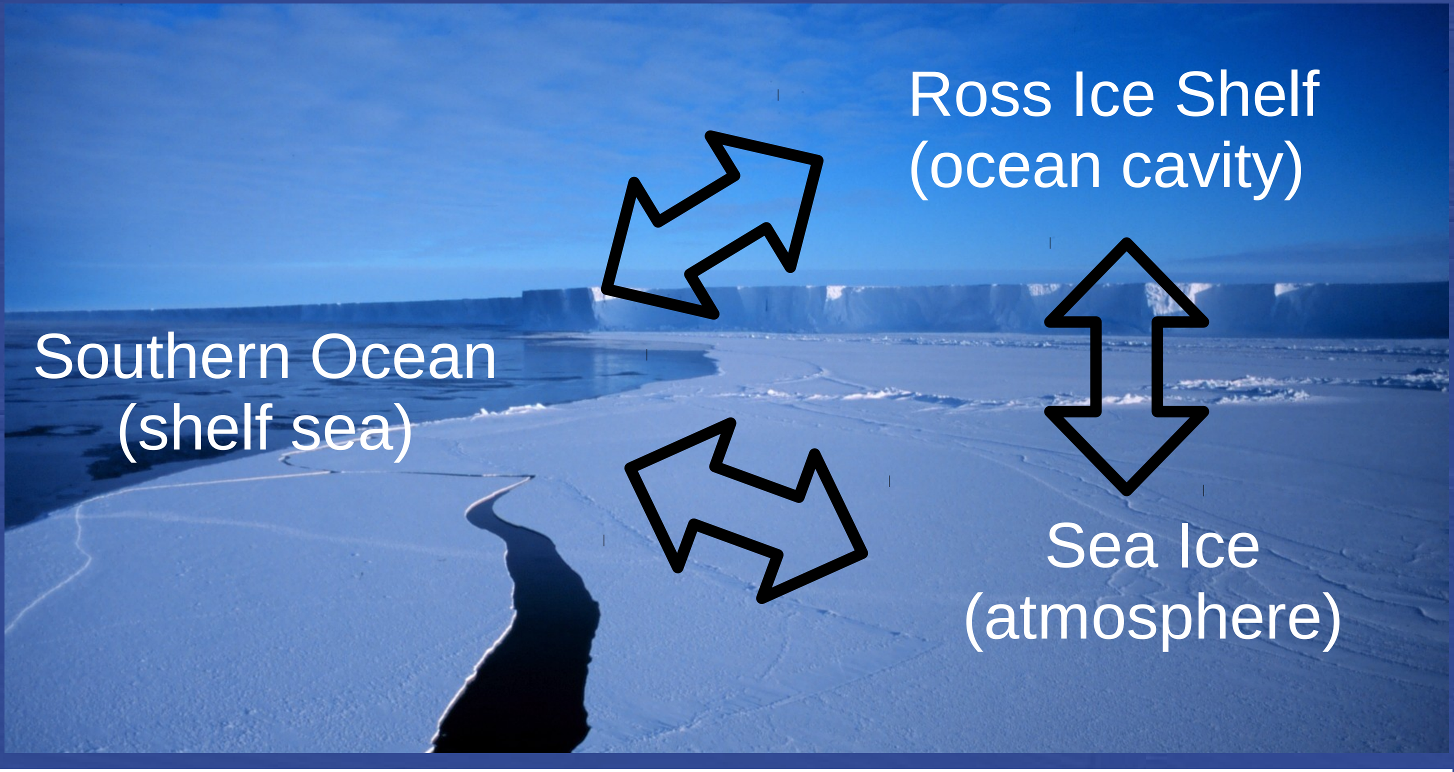

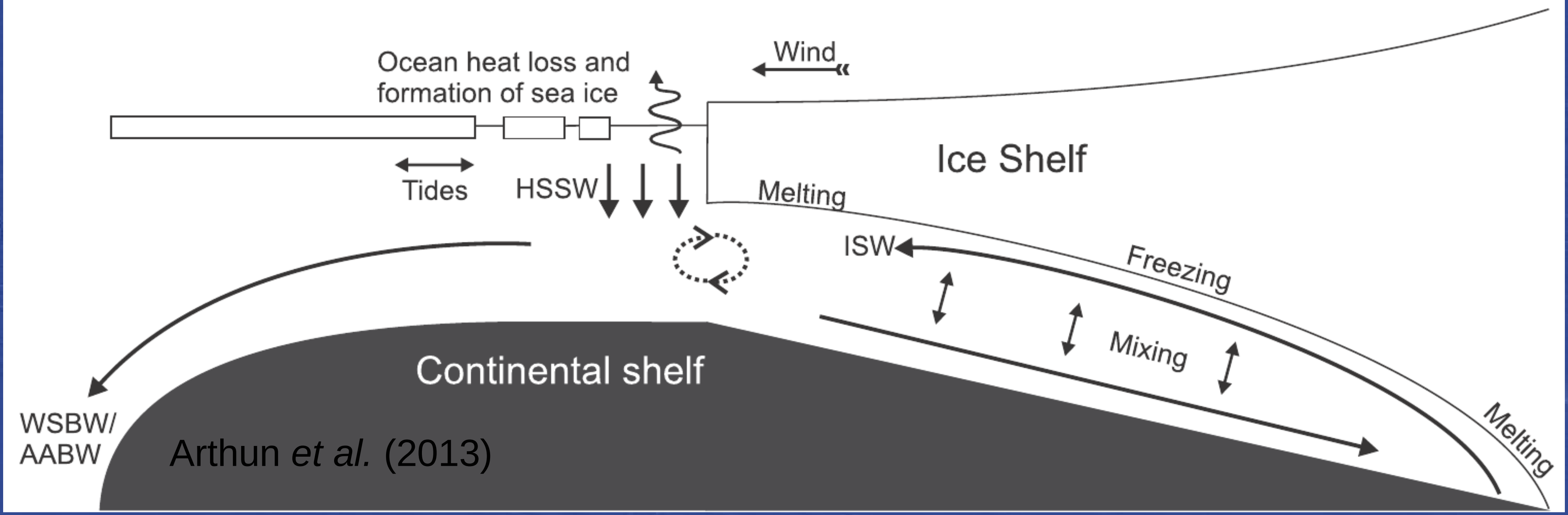

Arthun *et al.* (2013)

System Ice Shelf – Ocean – Sea Ice

- ocean currents in the Ross Sea
- ice shelf melting
- melt water plumes (Ice Shelf Water, ISW)
- platelet ice
- Antarctic Coastal Current, fresh water signal from the Amundsen Sea
- polynya ocean dynamics
- production & transport of High Salinity Shelf Water (HSSW)
- production of Antarctic Bottom Water (AABW)
- Antarctic Slope Current (ASC), on-shelf transport of MCDW
- phytoplankton blooms and sea ice
- exchange across the ice shelf front
- heat transport, mode 1 & 2 (HSSW & MCDW)

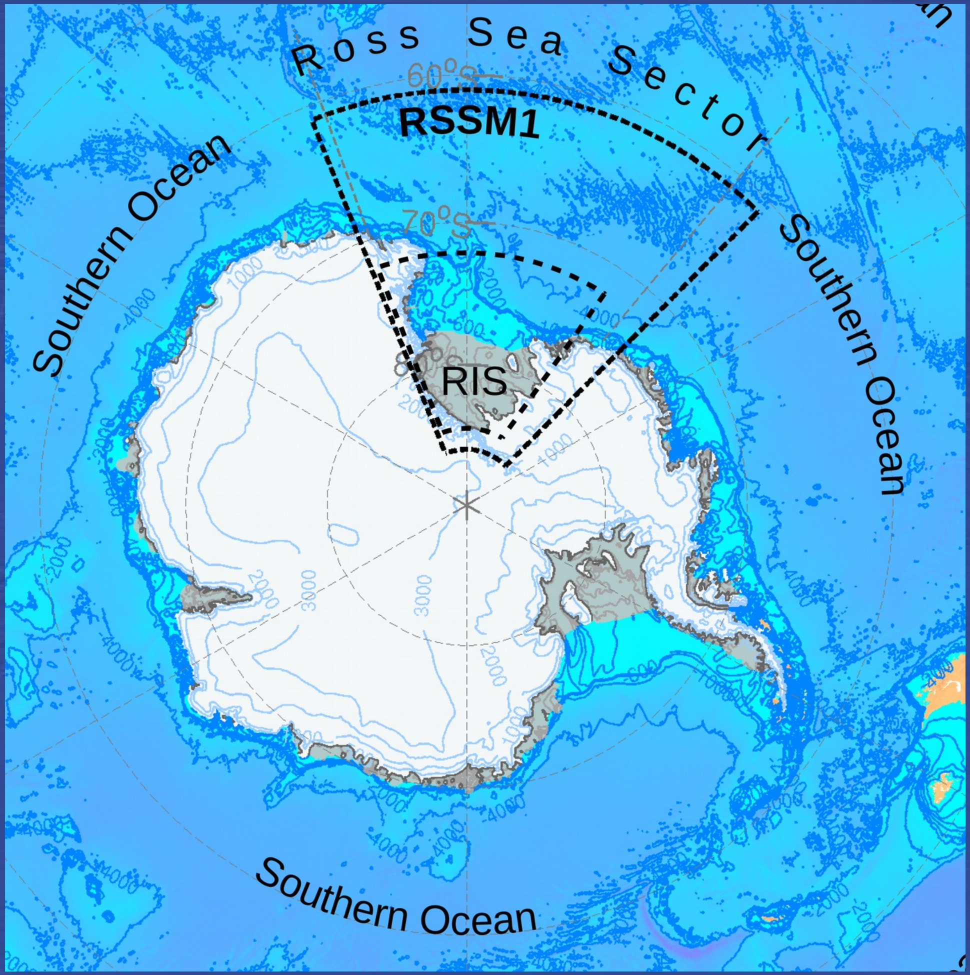

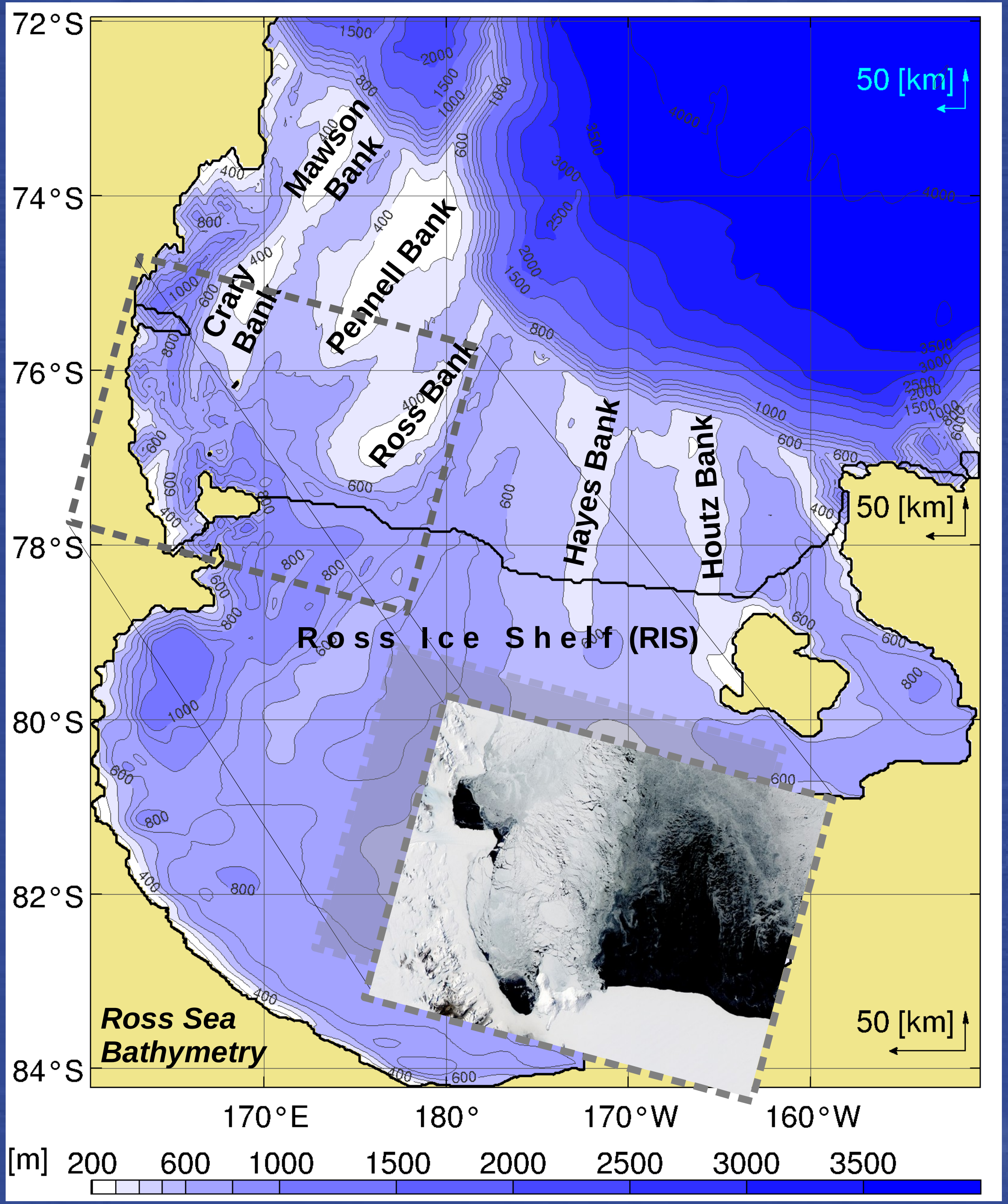

Ross Sea Sector Model 2 (RSSM2)

- climatological circulation model (ROMS)
- thermodynamic ice shelf-ocean coupled
- sea ice fluxes parameterized ← SSM/I
- surface heat flux ← NCEP
- T, S ← WOA09; momentum ← GODAS; tides ← TPXO7.2

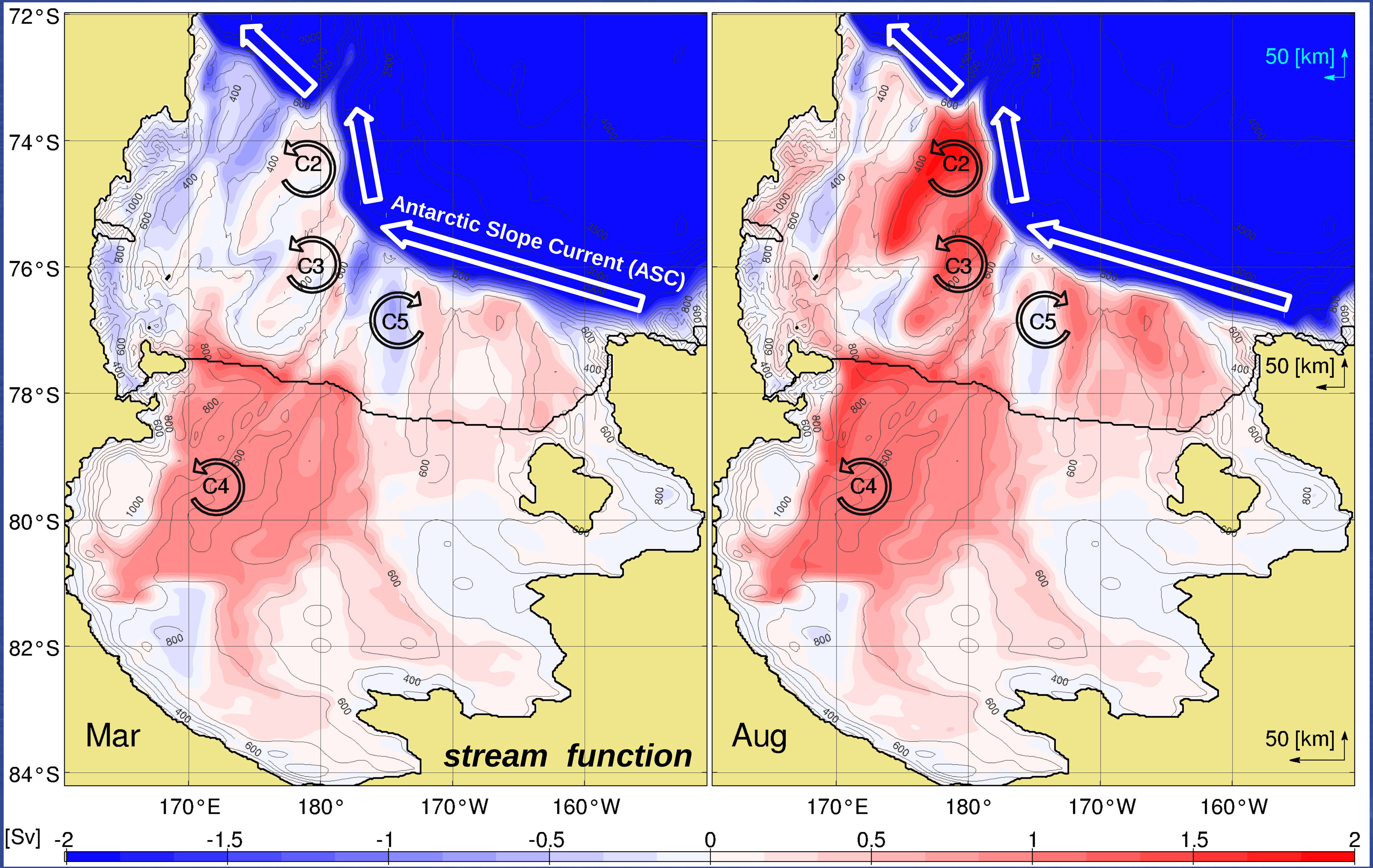
Antarctic Slope Current (ASC)
C2
C3
C4
C5
Mar
Aug
stream function
50 [km]
72°S
74°S
76°S
78°S
80°S
82°S
84°S
170°E
180°
170°W
160°W
[Sv]
-2
-1.5
-1
-0.5
0
0.5
1
1.5
2

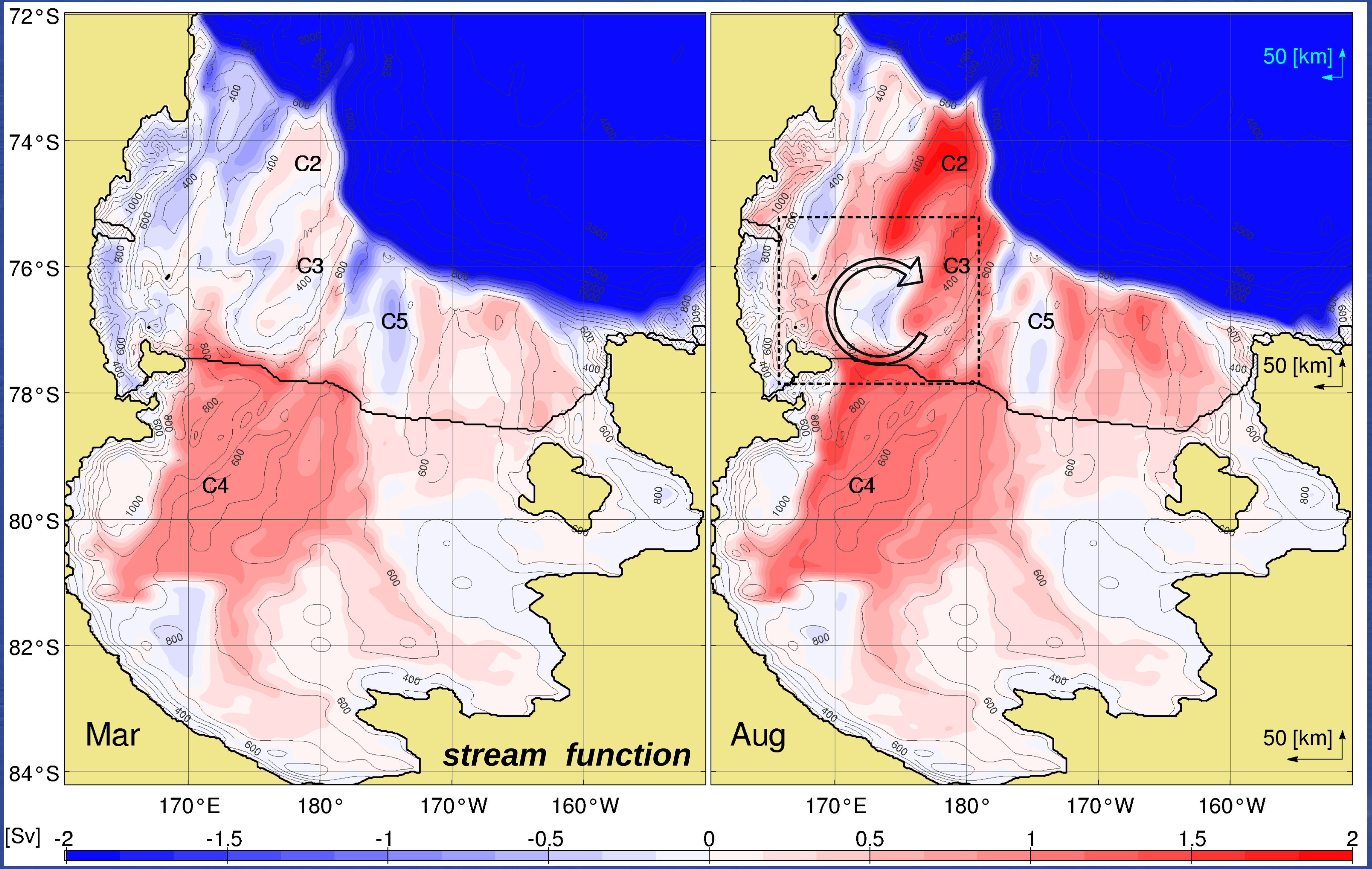

Mar
Aug
stream function
C2
C3
C4
C5
50 [km]
72°S
74°S
76°S
78°S
80°S
82°S
84°S
170°E
180°
170°W
160°W
[Sv]
-2
-1.5
-1
-0.5
0
0.5
1
1.5
2

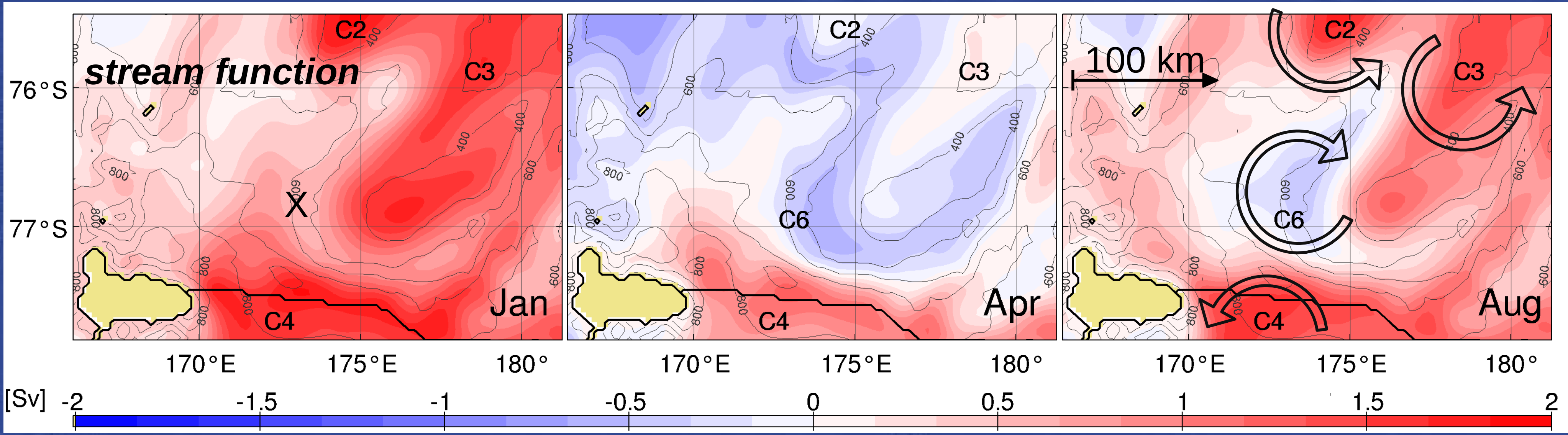

→ seasonal circulation cell C6 forms in April

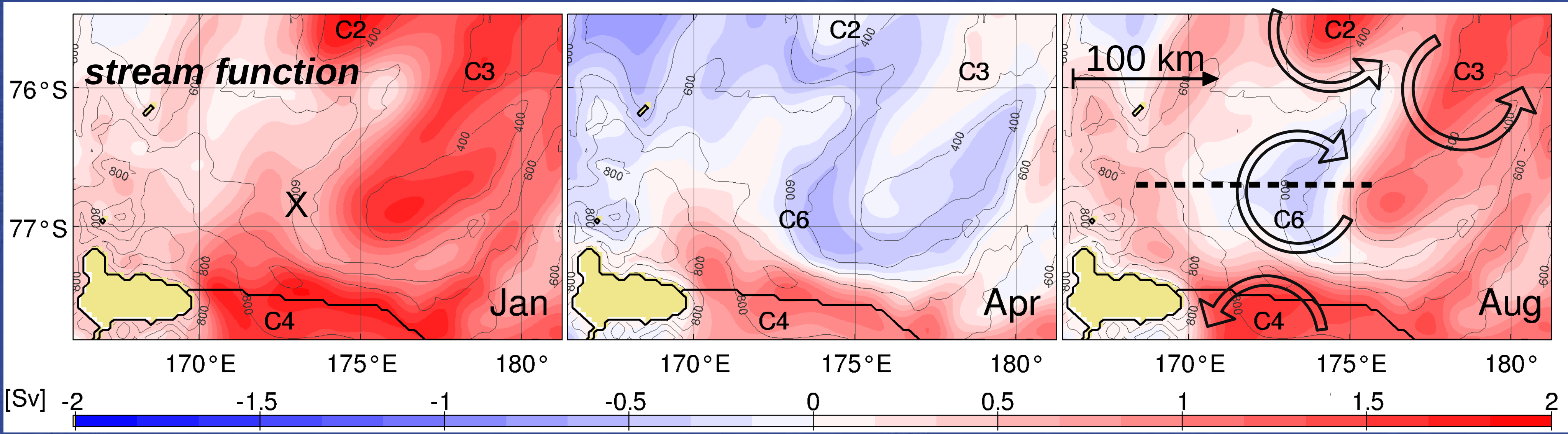

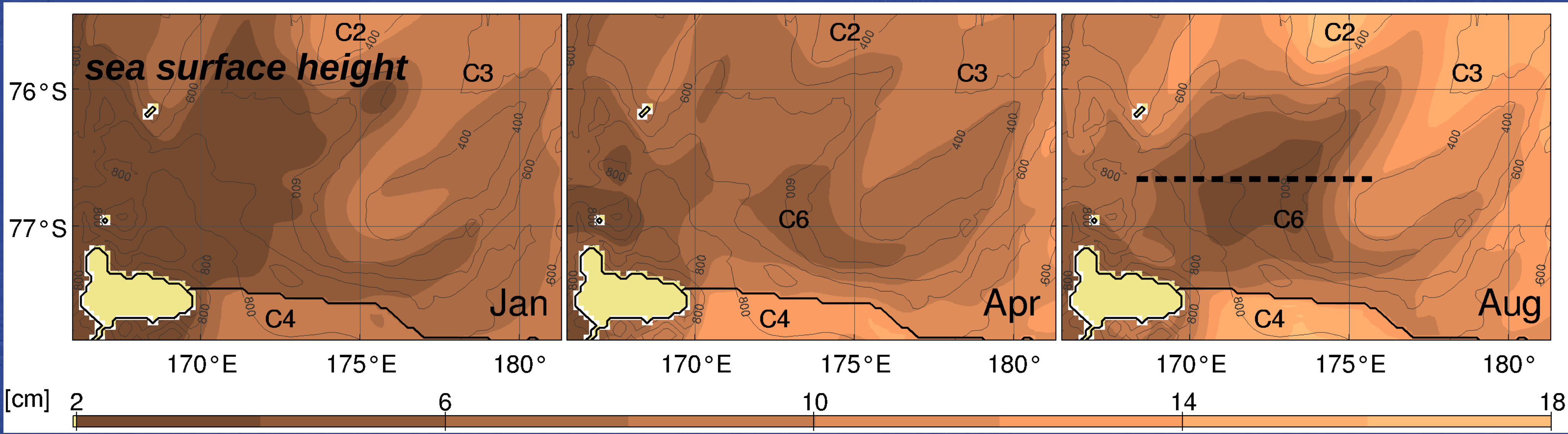

➔ seasonal circulation cell C6 forms in April

➔ C6 correlates with SSH depression

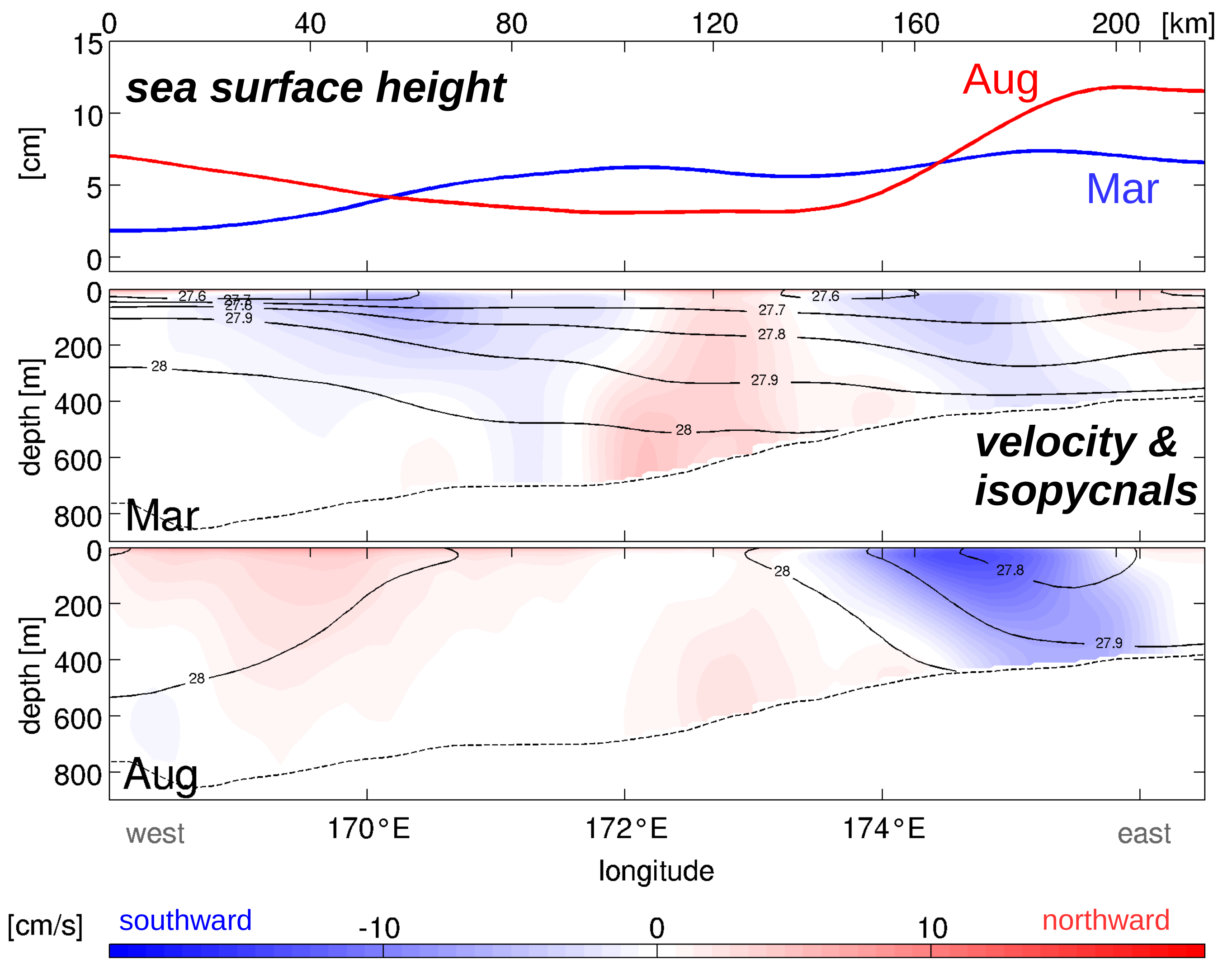
sea surface height
Aug
Mar
[cm]
[km]
velocity & isopycnals
depth [m]
Mar
Aug
west
170°E
172°E
174°E
east
longitude
[cm/s]
southward
northward
-10
0
10

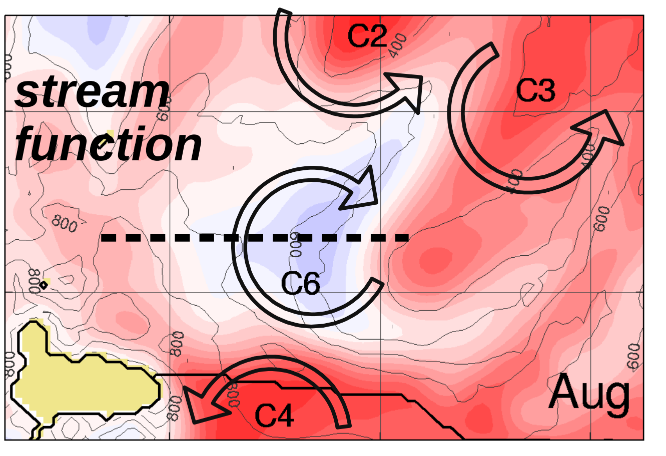
stream function
C2
C3
C6
C4
Aug

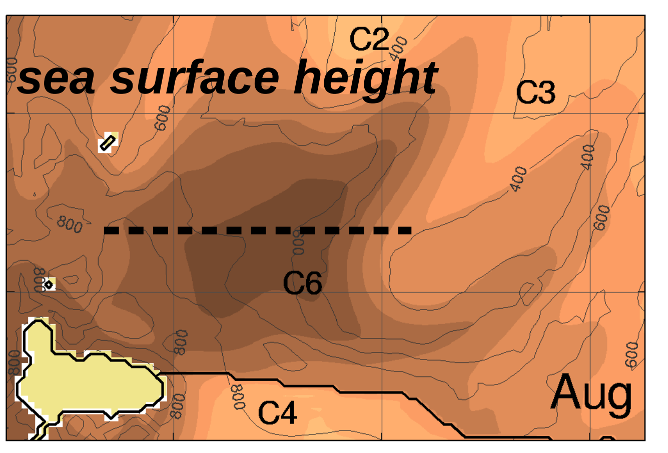
sea surface height
C2
C3
C6
C4
Aug

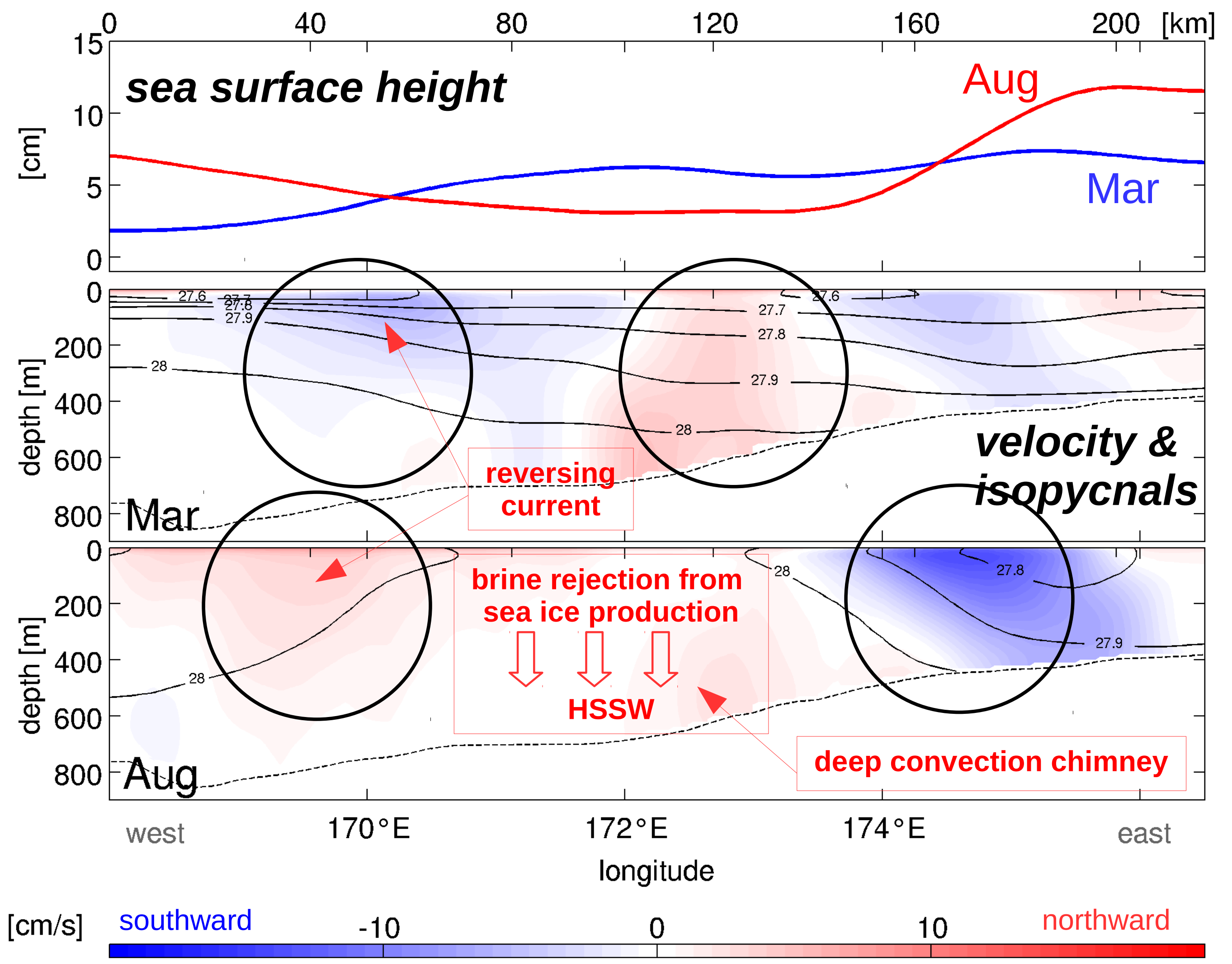

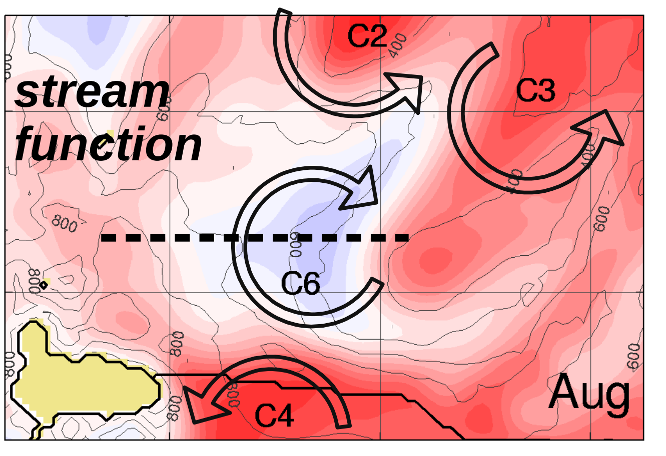

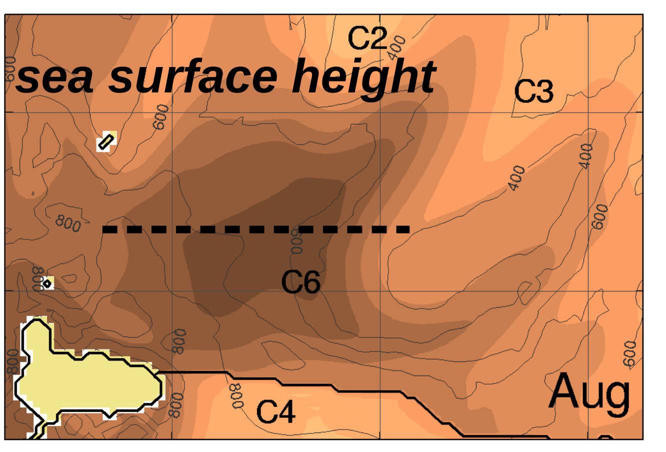

- ➔ August: brine rejection from sea ice production forms dense HSSW
- ➔ Relative SSH depression within the convection chimney
- ➔ SSH gradients cause barotropic geostrophic currents

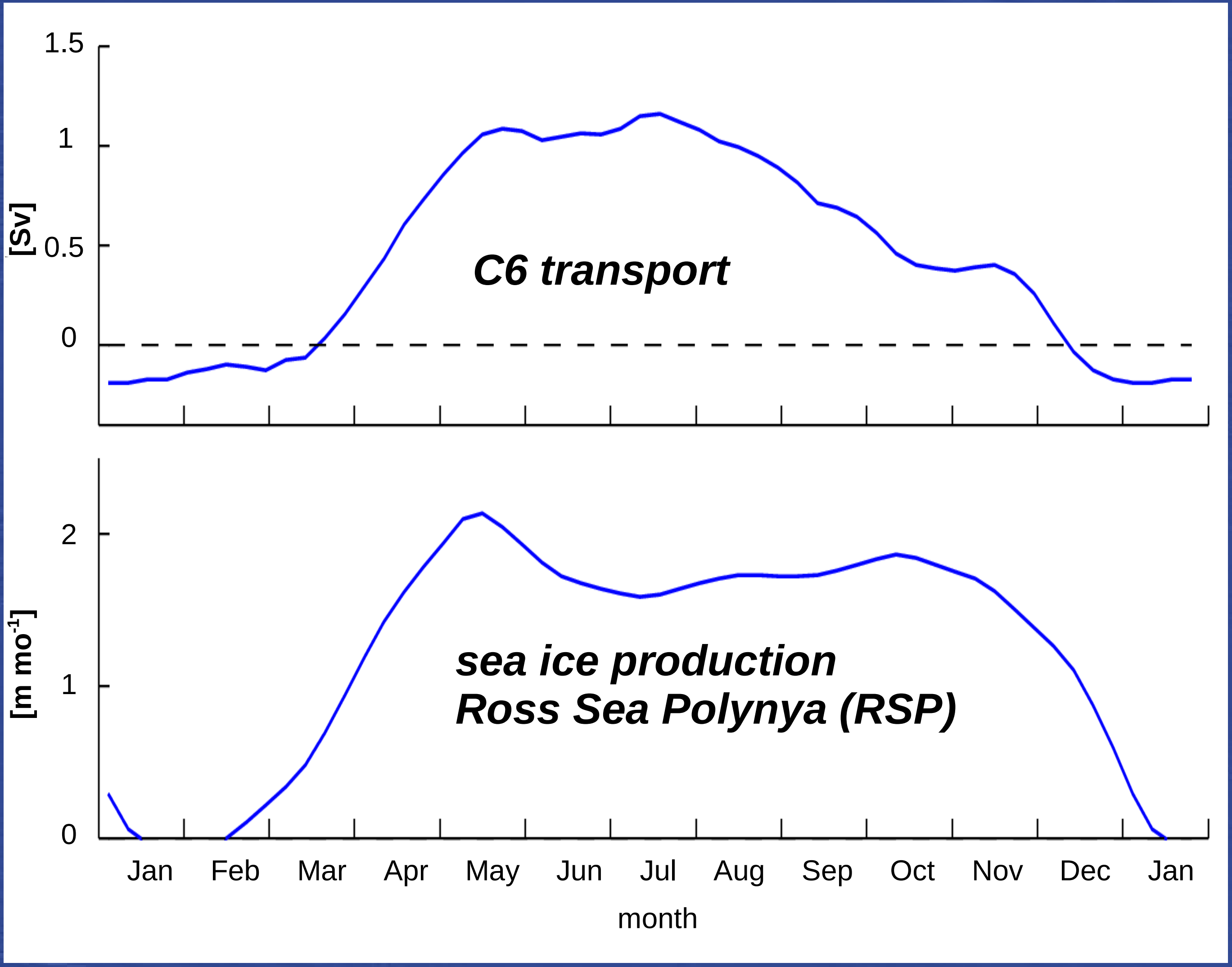

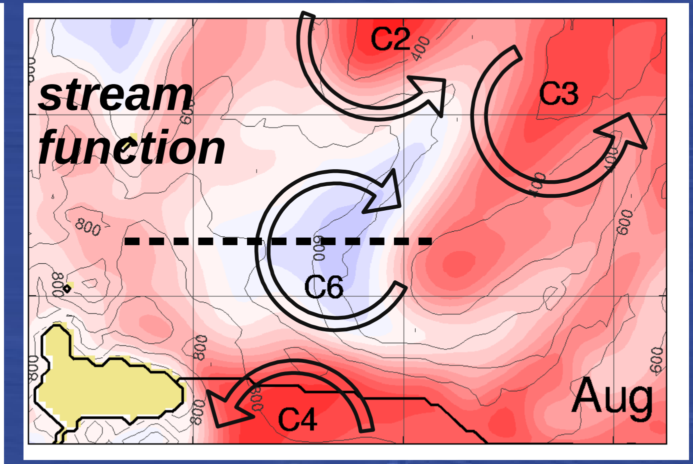

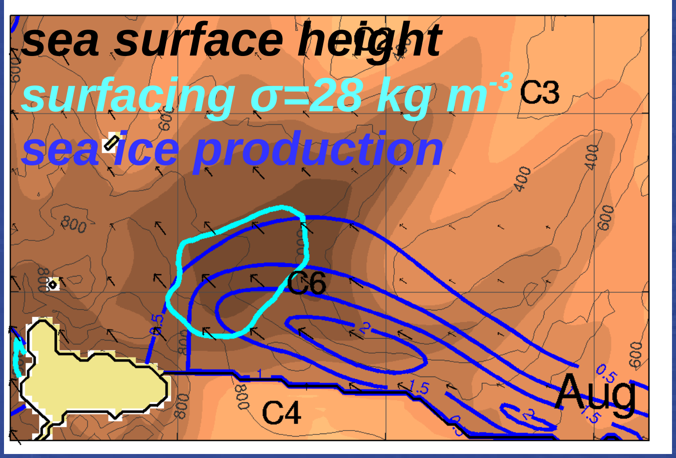

- Ekman Transport causes off set between polynya and deep convection → poster

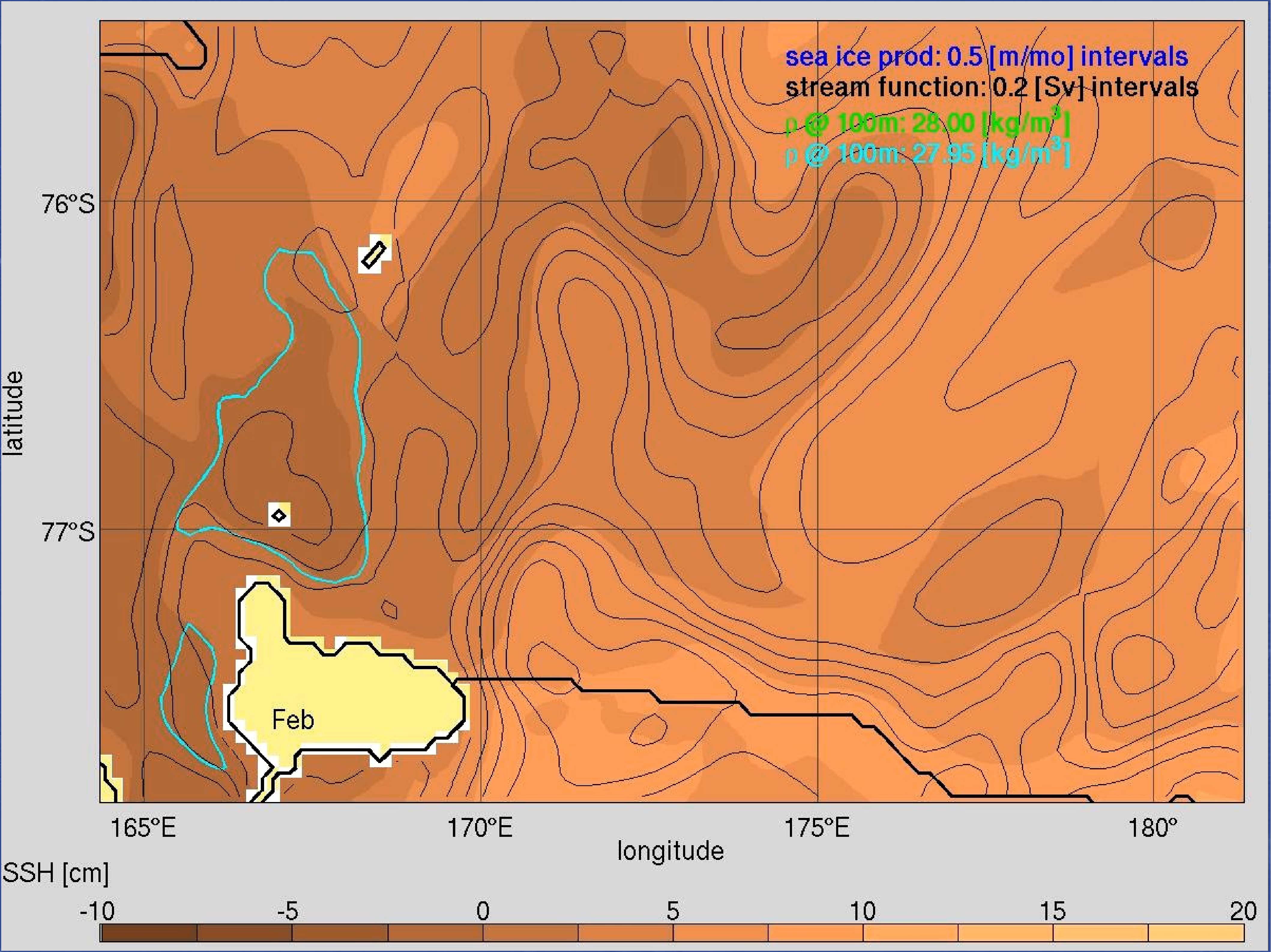
sea ice prod: 0.5 [m/mo] intervals
stream function: 0.2 [Sv] intervals
ρ @ 100m: 28.00 [kg/m3]
ρ @ 100m: 27.95 [kg/m3]
76°S
77°S
latitude
Feb
165°E
170°E
175°E
180°
longitude
SSH [cm]
-10
-5
0
5
10
15
20

Structure & Transports

- ➔ persistent and seasonal circulation cells over the continental shelf
- ➔ net transports up to ~2 Sv | anomalies > 50% → poster

Drivers

- ➔ lateral density gradients (between CDW, HSSW, ISW) → poster
- ➔ momentum from the ASC → poster
- ➔ sea ice: *RSP eddy* (C6) is a direct consequence of the Ross Sea Polynya
  - mechanism is a *rim current* (Chapman 1998). representation in ROMS?
  - non neglectable circulation feature in polar oceans

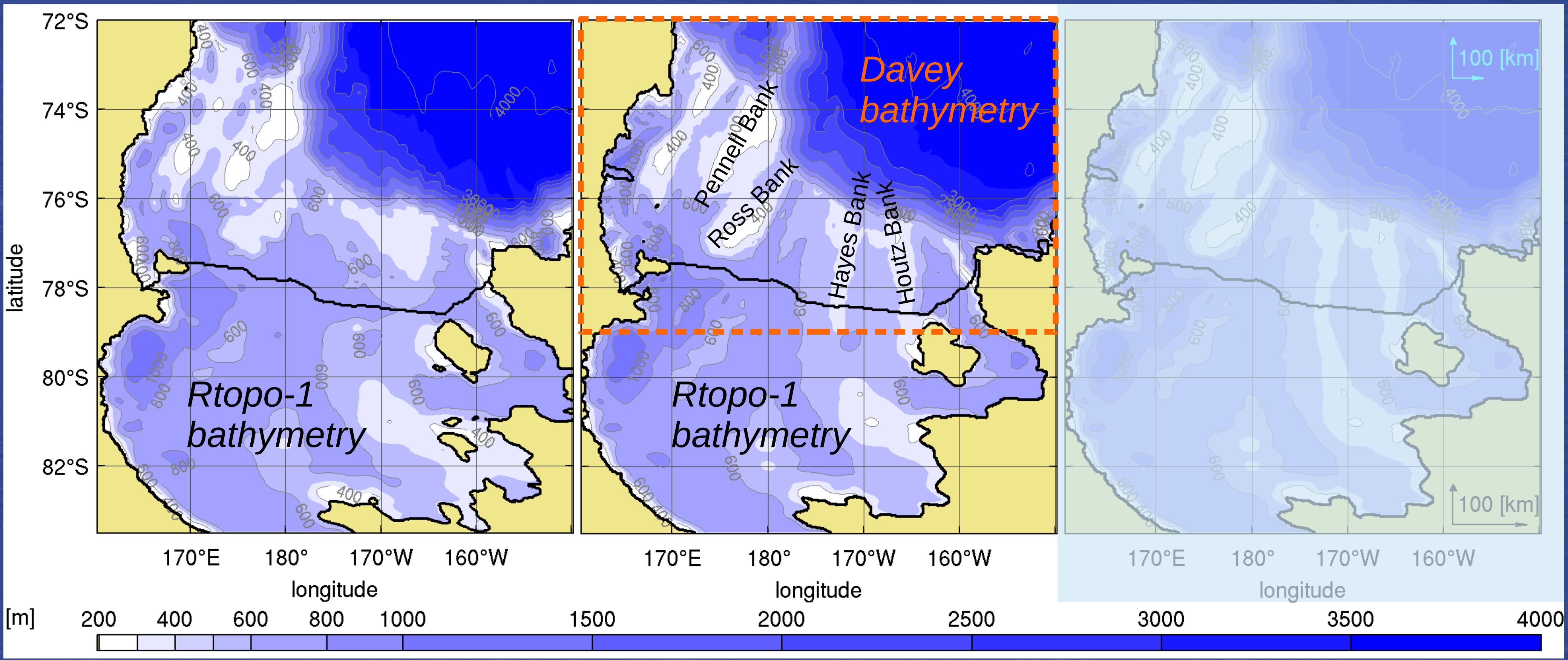

- Davey, F. (2004). Ross Sea Bathymetry, 1:2,000,000, version 1.0, Institute of Geological & Nuclear Sciences geophysical map 16.
- Davey, F. and Nitsche, F. (2005). Bathymetric grid of the Ross Sea, Antarctica.

- Timmermann, R., Le Brocq, A. M., Deen, T., Domack, E., Dutrieux, P., Galton-Fenzi, B. K., Hellmer, H. H., Humbert, A., Jansen, D., Jenkins, A., Lambrecht, A., Makinson, K., Niederjasper, F., Nitsche, F., Nøst, O. A., Smedsrud, L. H., and Smith, W. H. F. (2010). A consistent dataset of Antarctic ice sheet topography, cavity geometry, and global bathymetry. Earth System Science Data Discussions, 3 (2), 231–257.

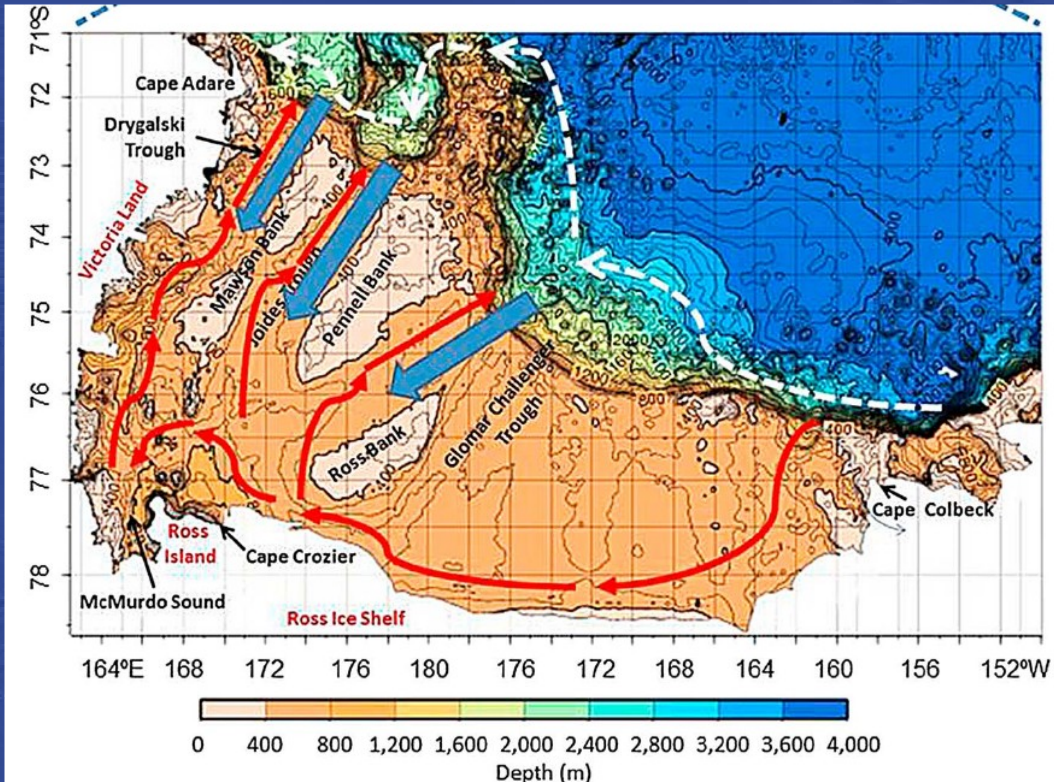

Smith, W. O., Dinniman, M. S., Hofmann, E. E., & Klinck, J. M. (2014). The effects of changing winds and temperatures on the oceanography of the Ross Sea in the 21st century. Geophysical Research Letters, 41(5), 1624–1631.

Smith, Walker O., J., Ainley, D. G., & Arrigo, K. R. (2014). The Oceanography and Ecology of the Ross Sea. Annual Review of Marine Science, 6, 469–87.

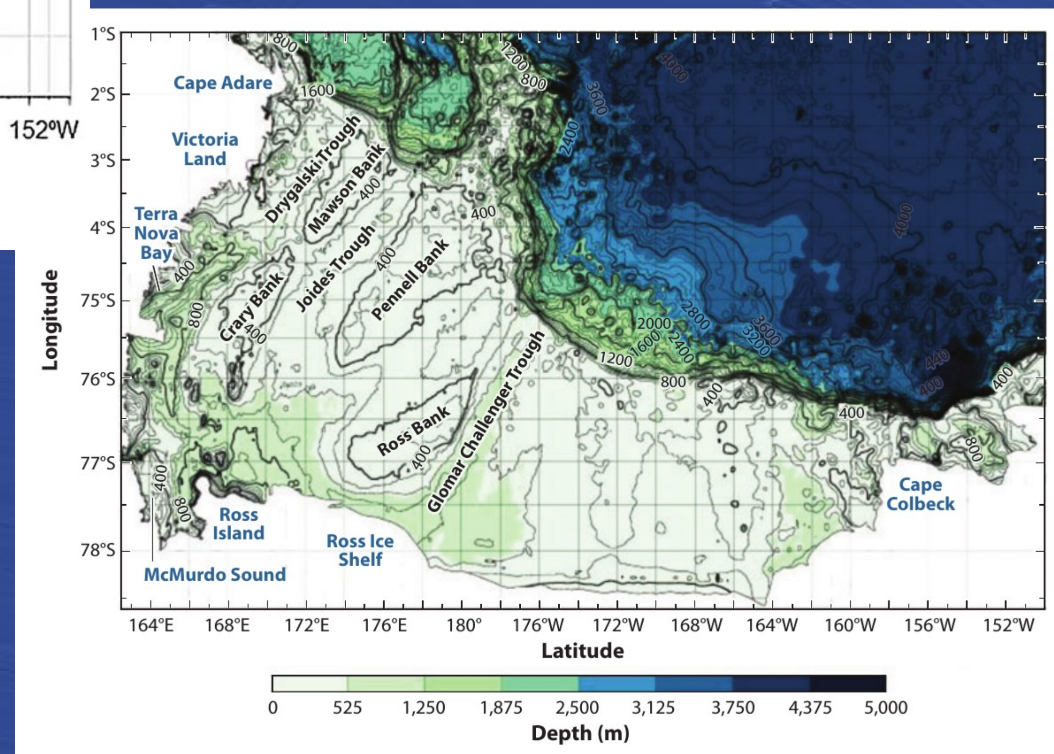

Figure 1

Bathymetric map of the Ross Sea. Based on the ETOPO1 bathymetry, with a contour interval of 100 m.

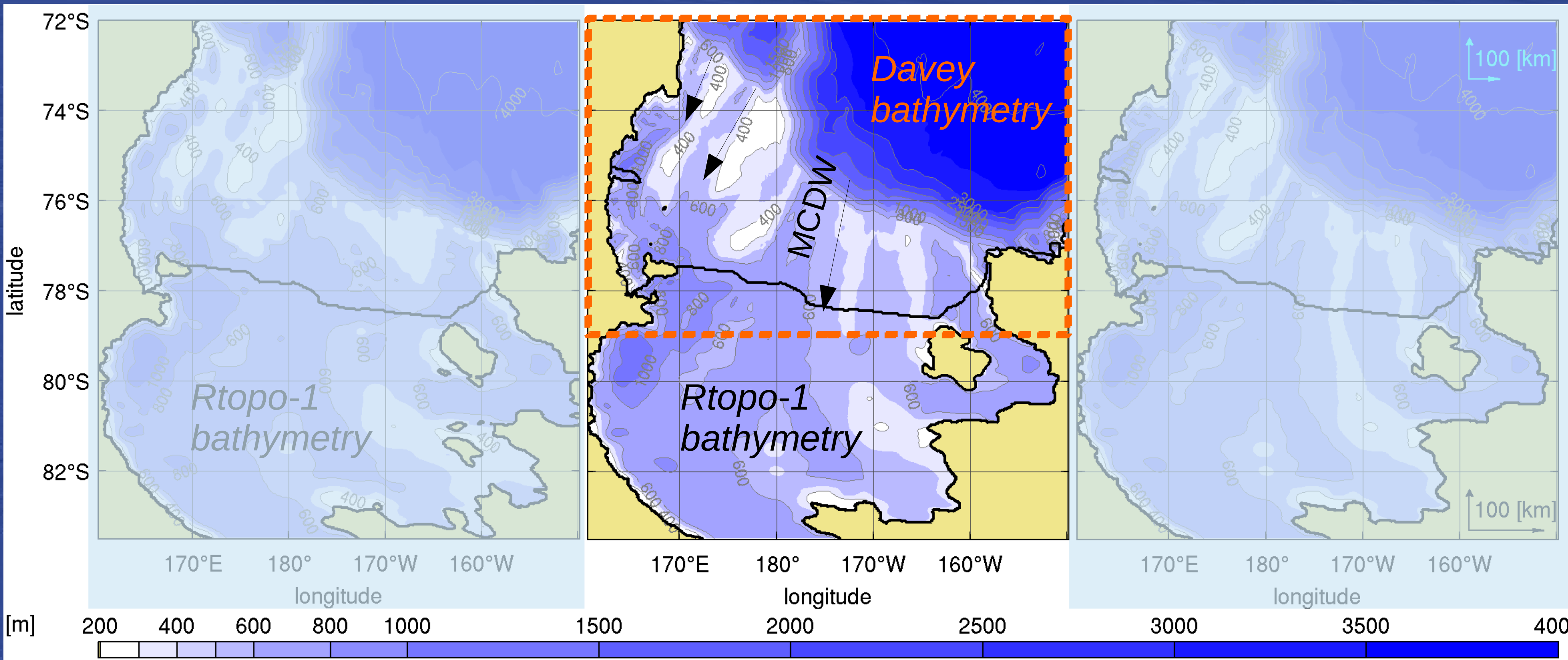

- MCDW is advected south along the western bank slopes
- Hayes Bank terminates where the two bathymetry merge

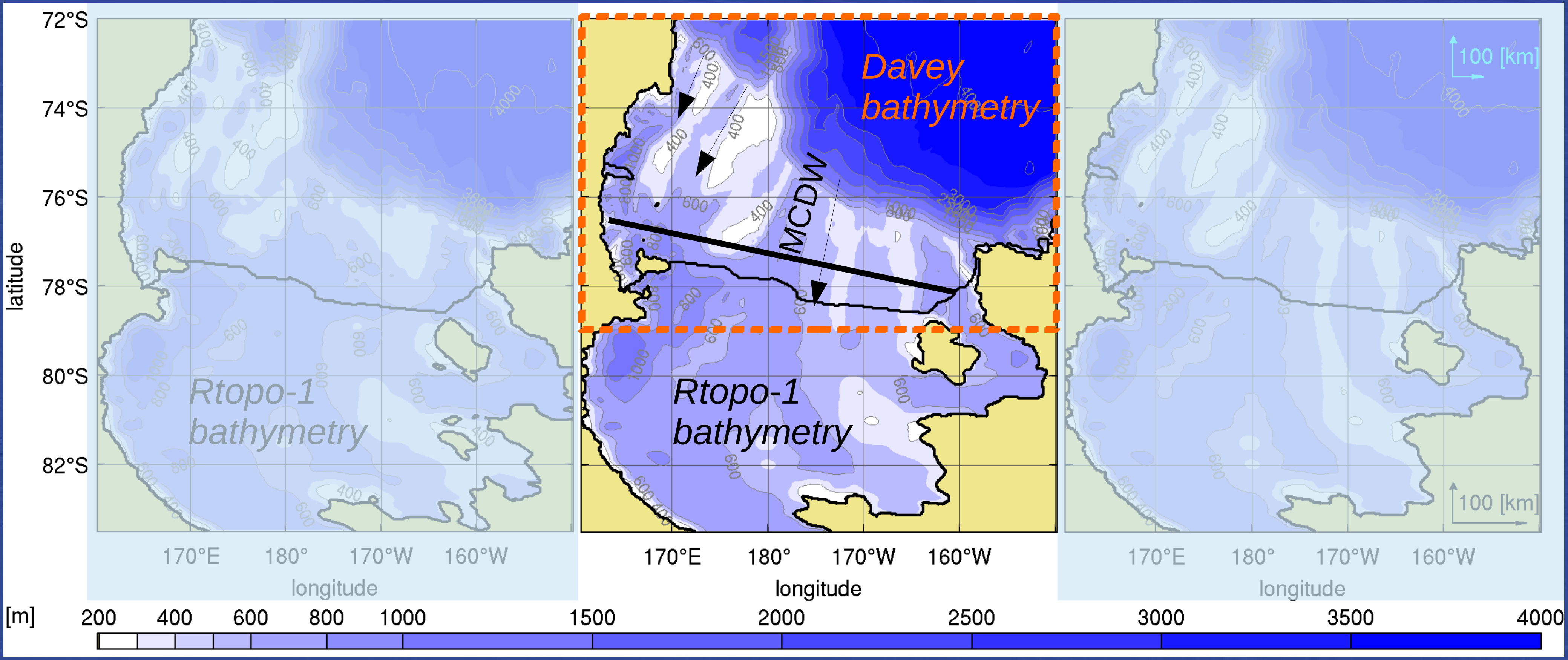

- MCDW is advected south along the western bank slopes
- Hayes Bank terminates where the two bathymetry merge

- MCDW @ 200-300m
- no HSSW observed over the eastern Ross Sea (Little America Basin)
- Why in the model(S!)

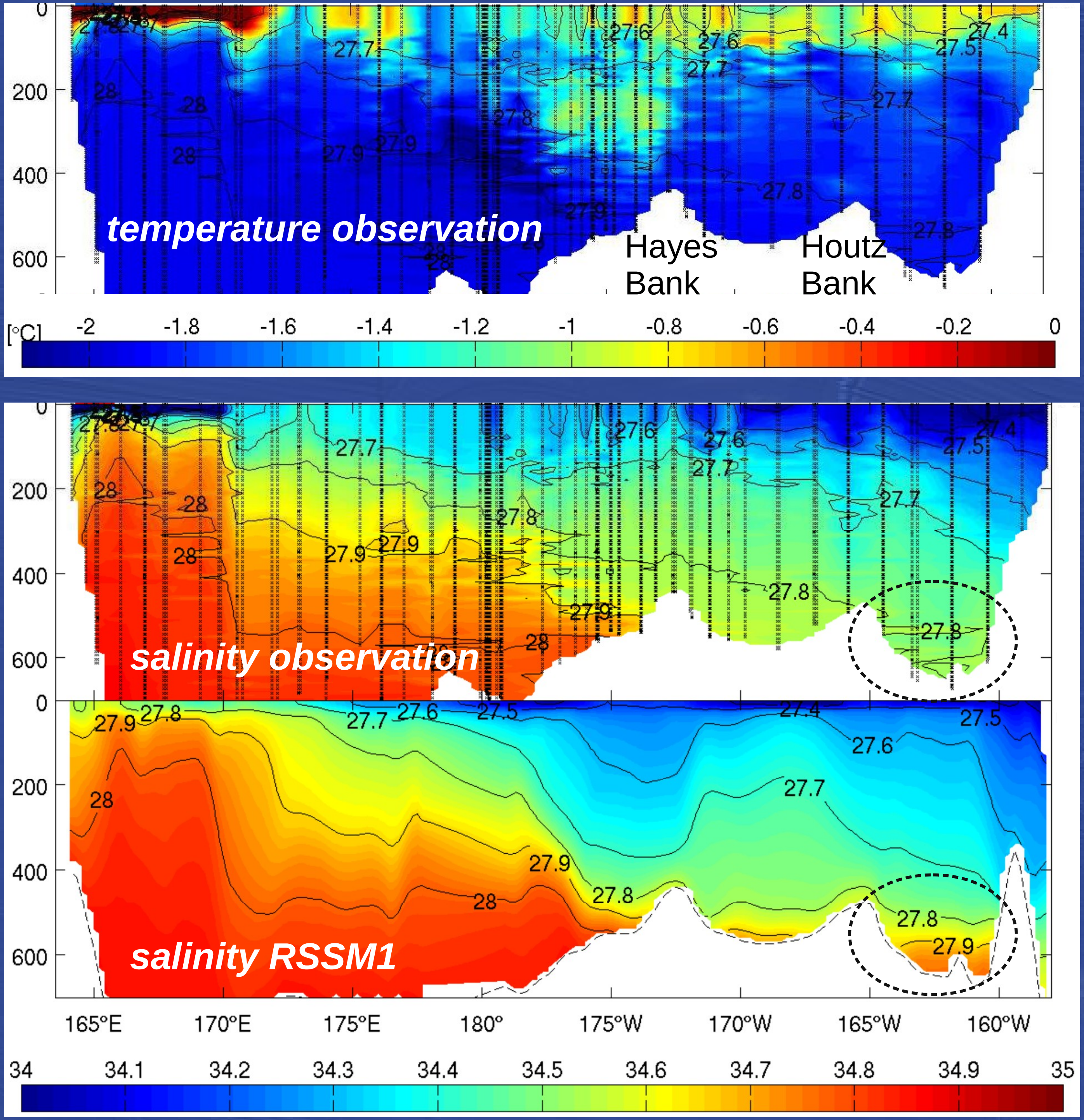

HSSW analysis

- ➔ HSSW in Glomar Challenger Basin has transited the cavity
- ➔ transit times ~ 2 years
- ➔ No southward flow of HSSW from Terra Nova Bay
- ➔ HSSW is not formed over the eastern shelf
- ➔ HSSW produced in polynyas, advected through the western cavity, passing via south of Hayes Bank → mode 1

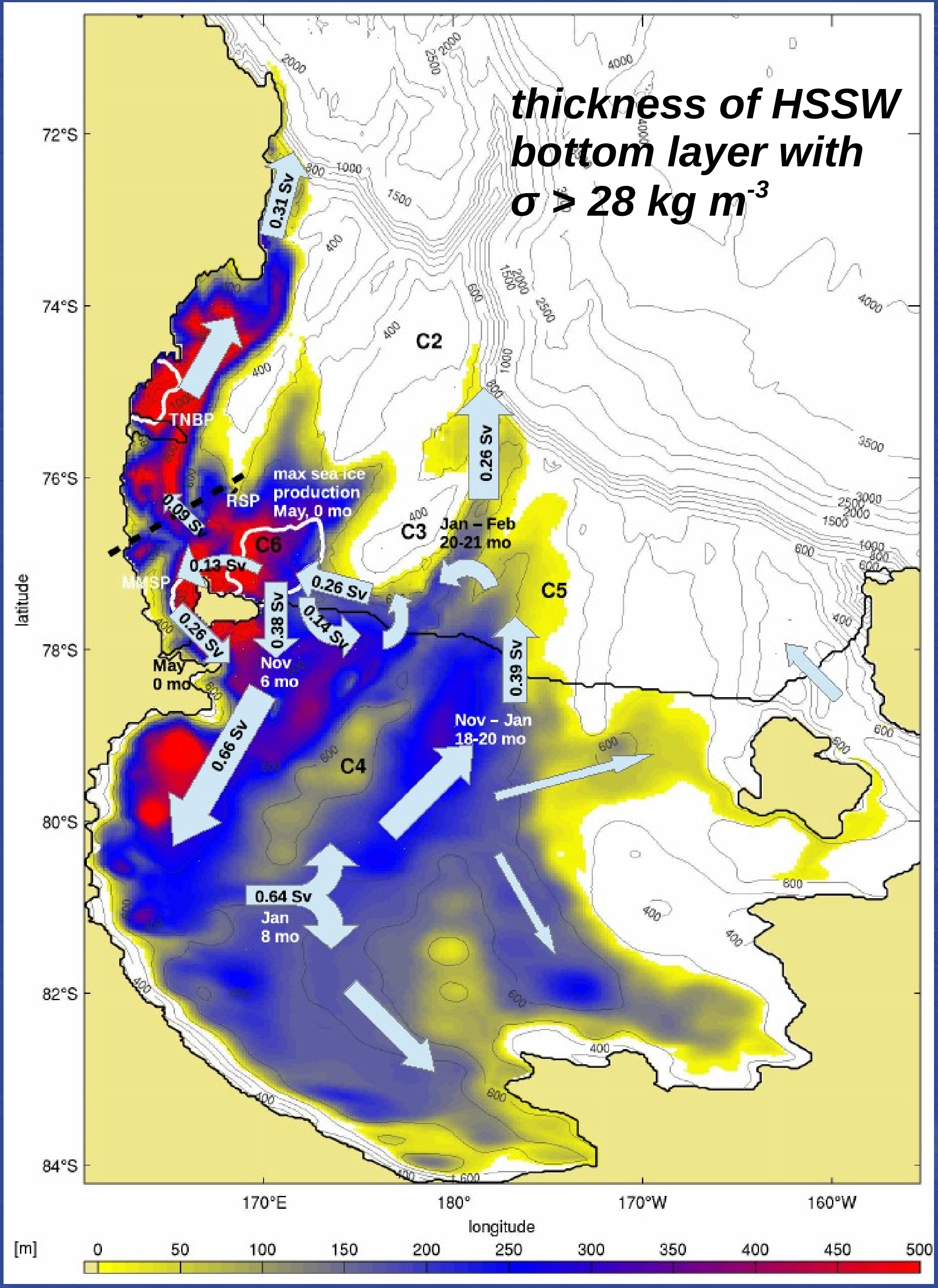

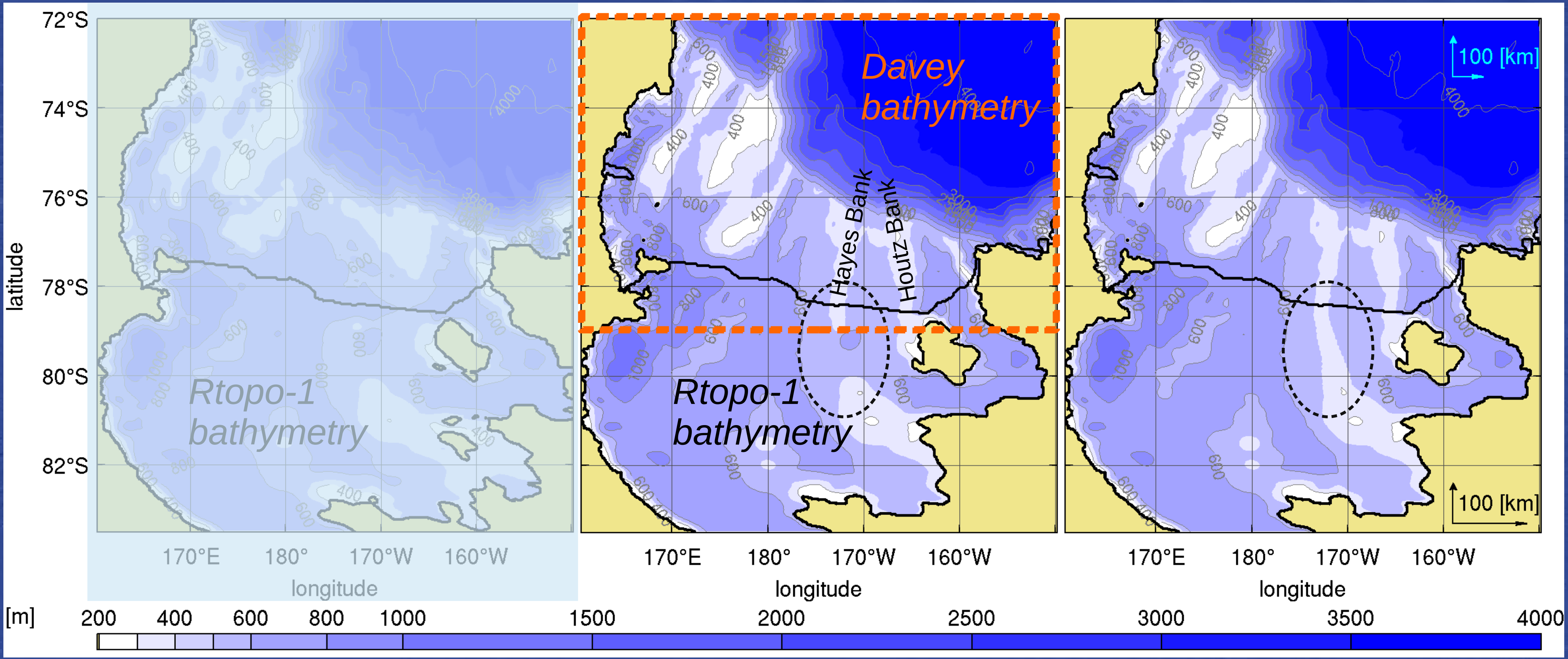

- Let's play :)
- Geo-engineered new Hayes Bank

RSSM1

RSSM1 bathym. experim.

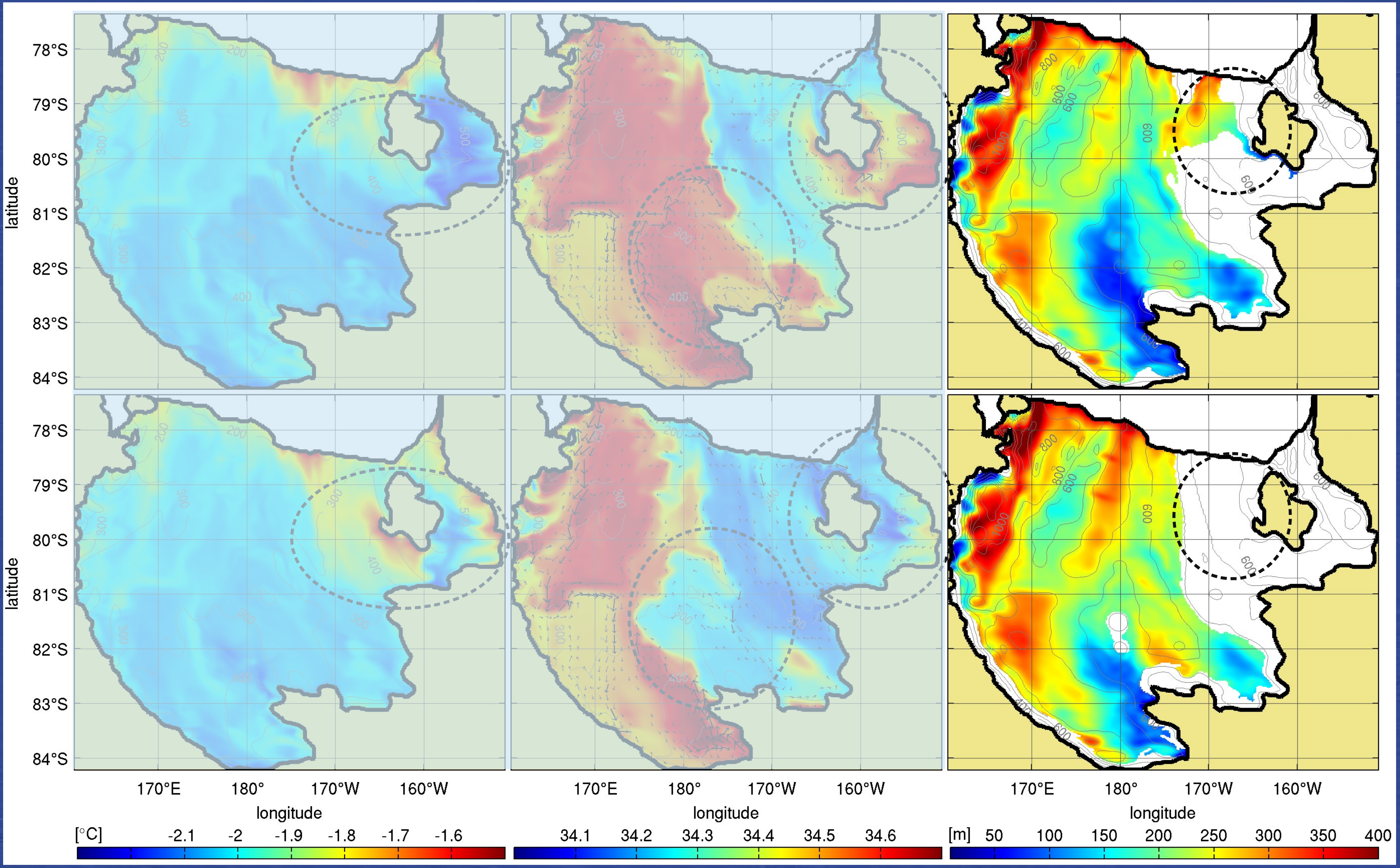

thickness of HSSW bottom layer with $\sigma > 28$ kg m^{-3}

RSSM1

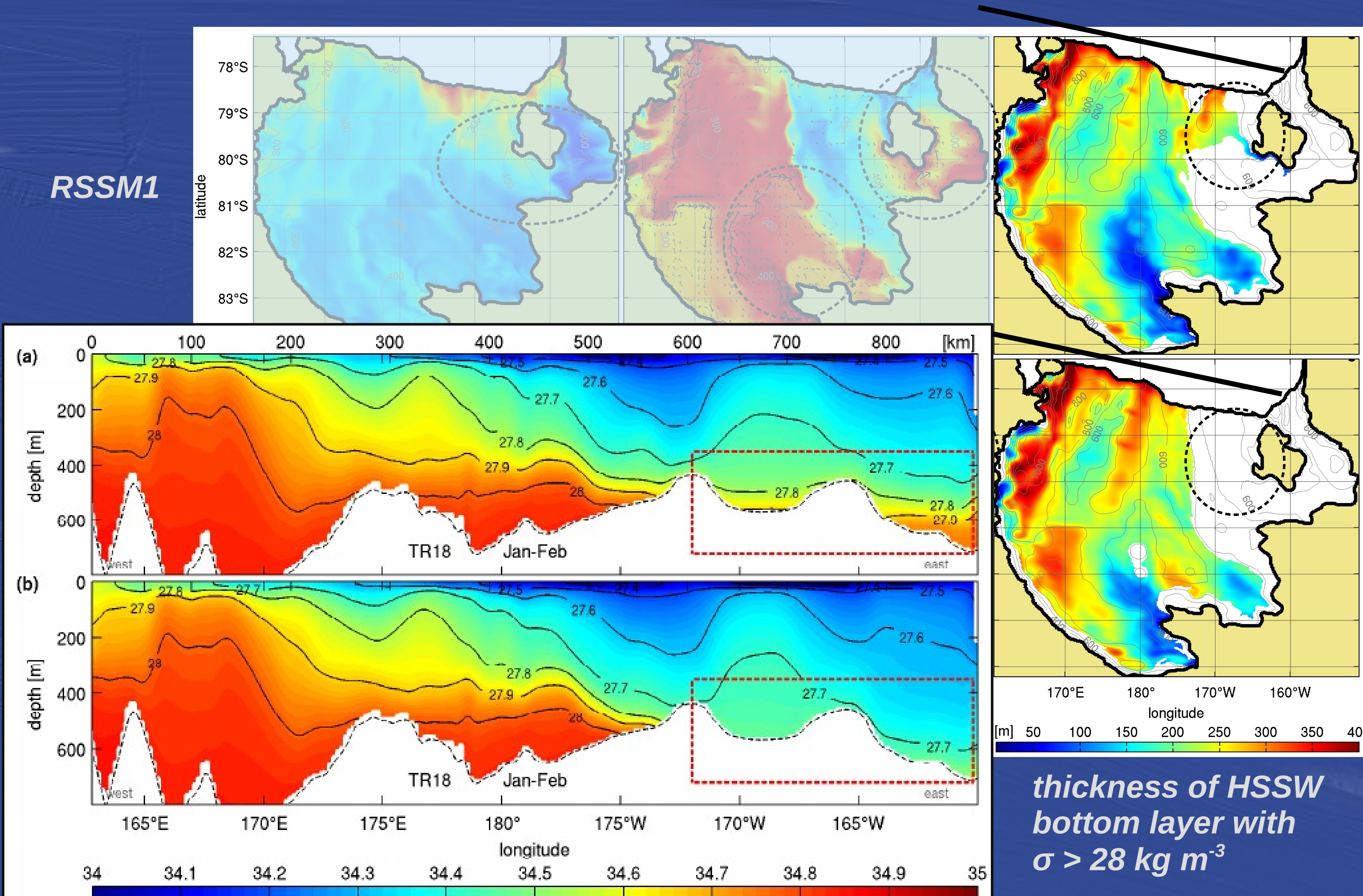

thickness of HSSW bottom layer with σ > 28 kg m^{-3}

RSSM1

RSSM1 bathym. experim.

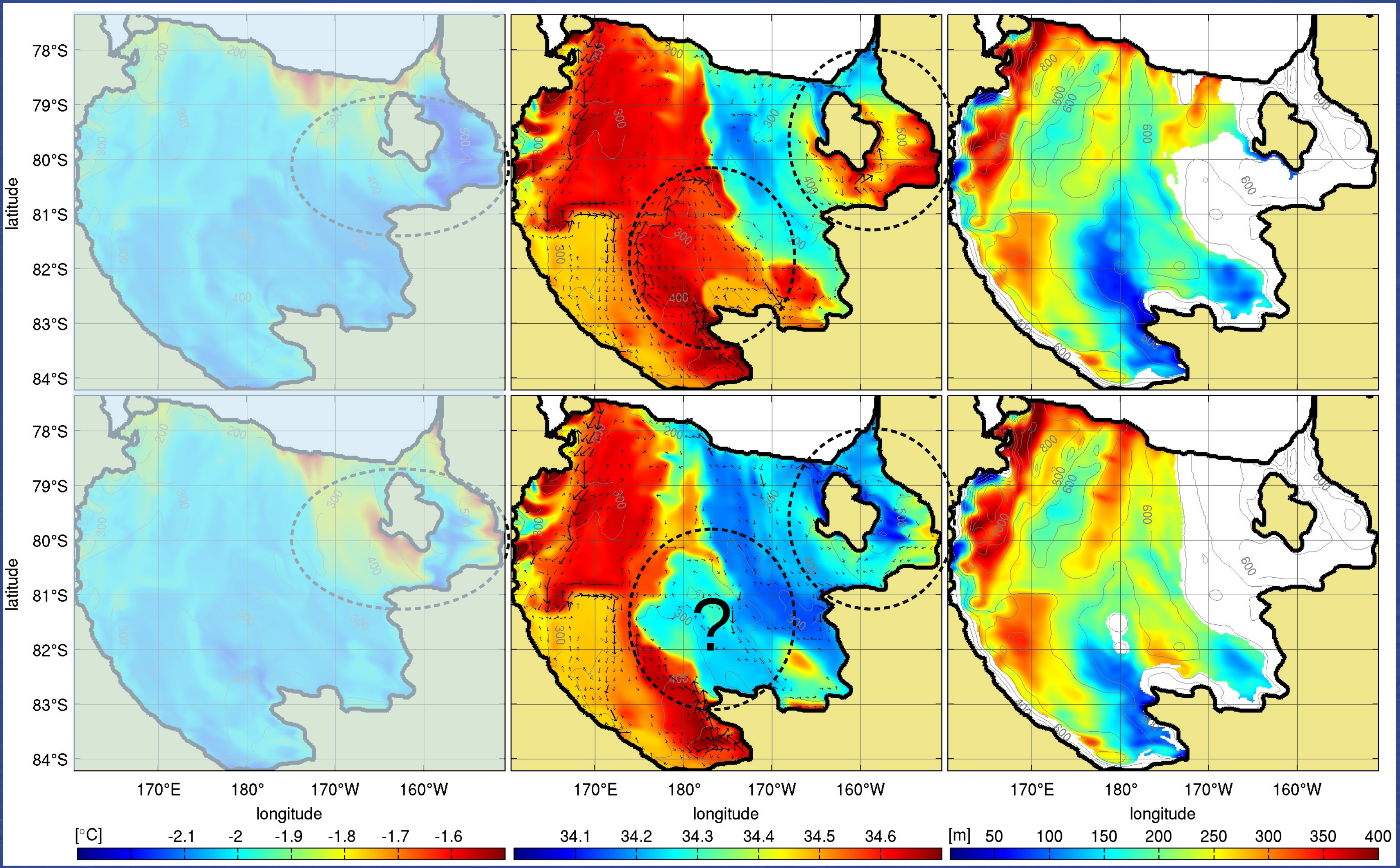

average salinity in the top 20 m

thickness of HSSW bottom layer with σ > 28 kg m^{-3}

RSSM1

RSSM1 bathym. experim.

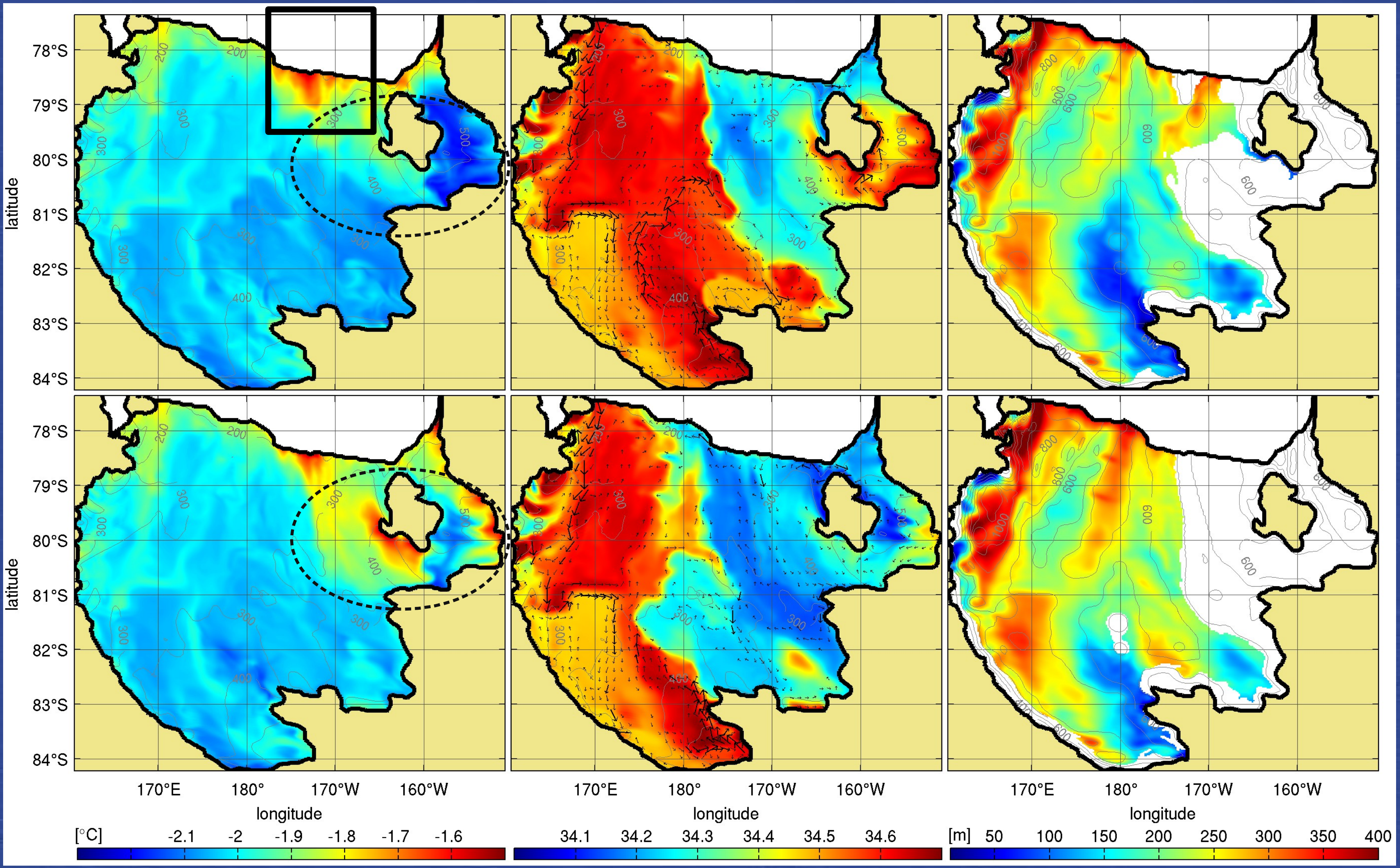

average temperature In the top 20 m

average salinity in the top 20 m

thickness of HSSW bottom layer with σ > 28 kg m^{-3}

mode 2 heat transport

➔ warm water passes the ice front

1. on surfaces of equal pot. Vort.

$$\Pi = \frac{f+\omega}{\rho} \cdot \nabla\lambda$$

2. along density slopes that run perpendicular to the ice edge

➔ the particular density structure is bound to the top of Hayes Bank

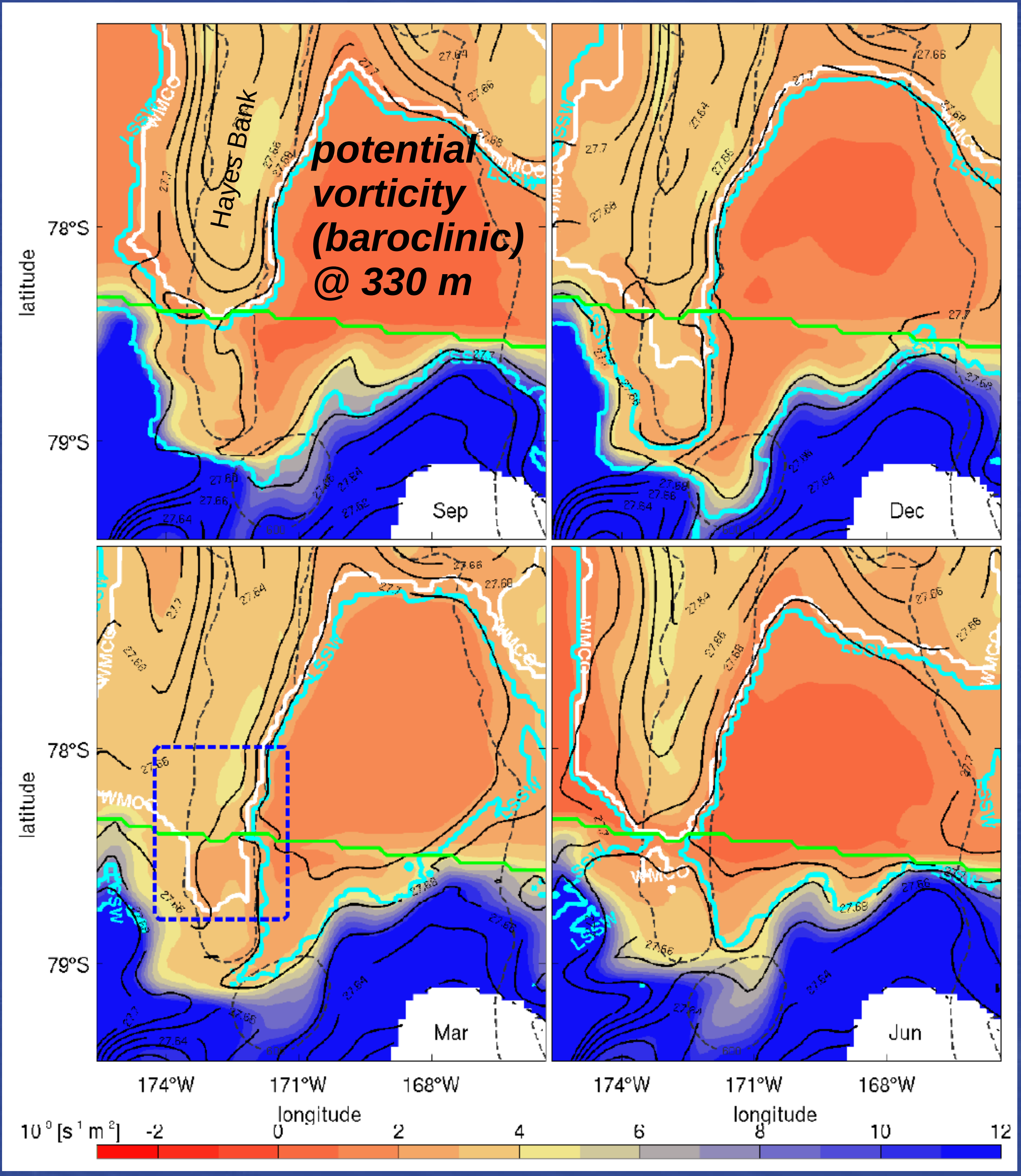

mode 2 heat transport
➔ warm water passes the ice front

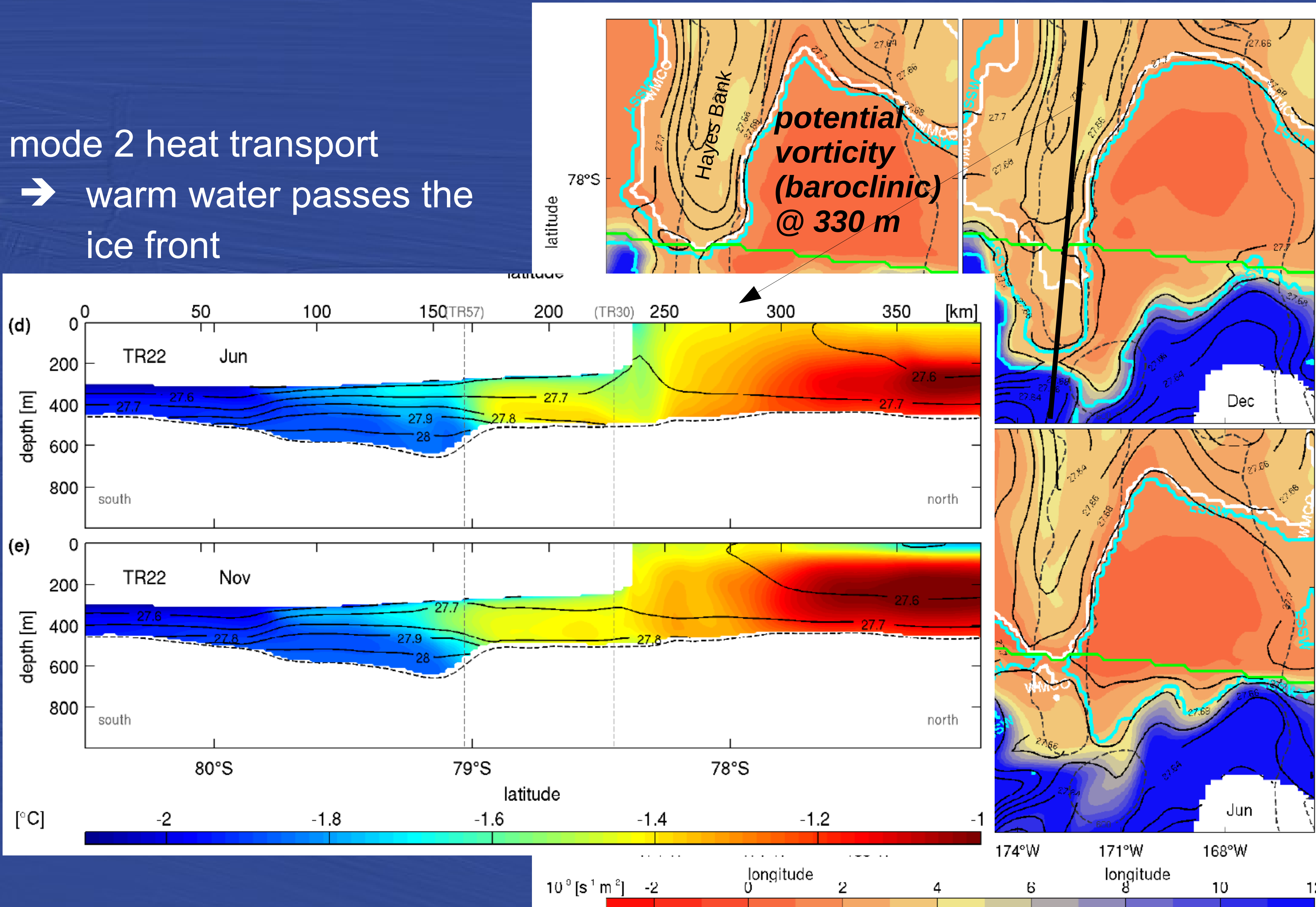

RSSM1

RSSM1 bathym. experim.

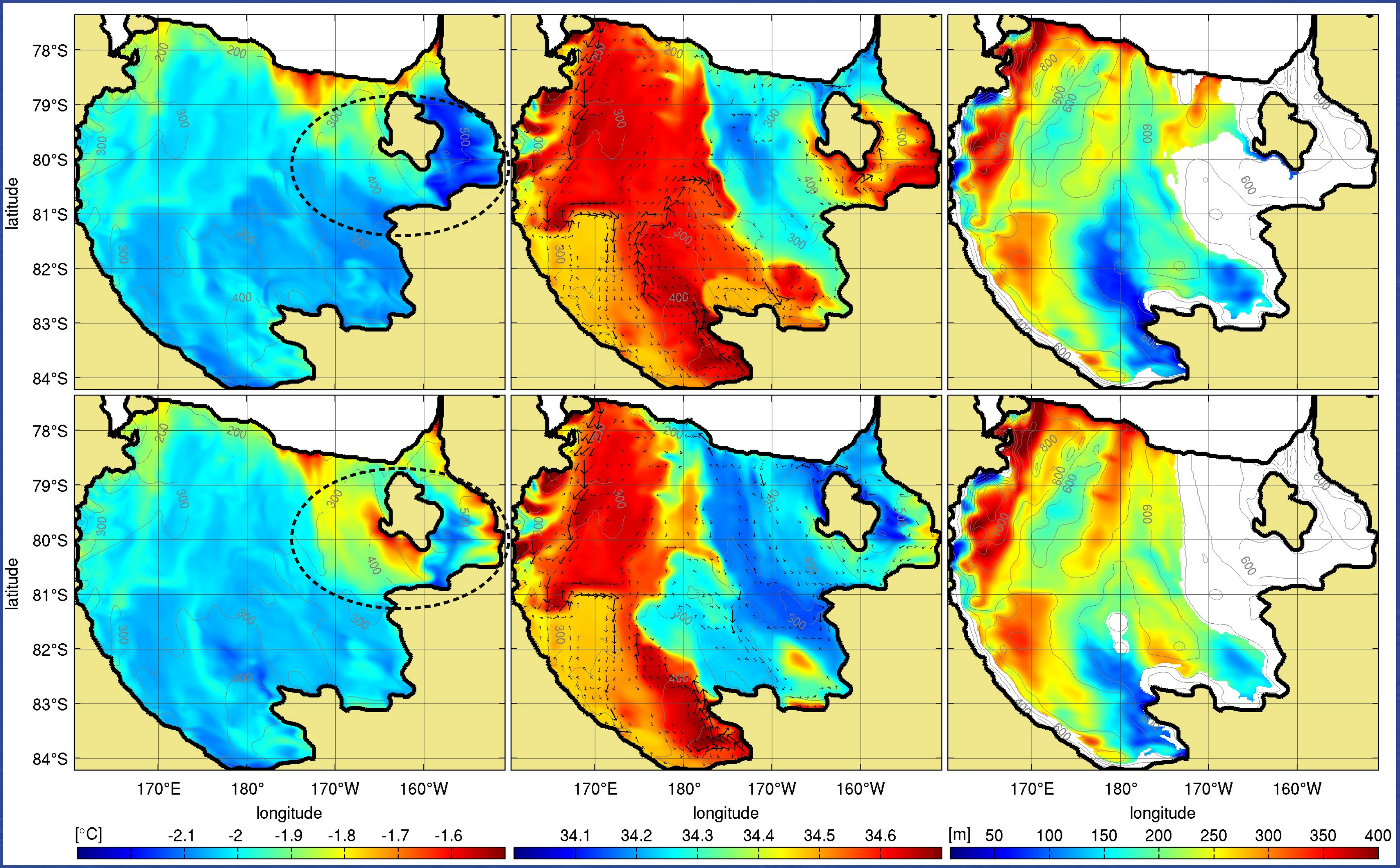

average temperature In the top 20 m

average salinity in the top 20 m

thickness of HSSW bottom layer with $\sigma > 28$ kg m^{-3}

More clutter from the dark ages of 'thesis'

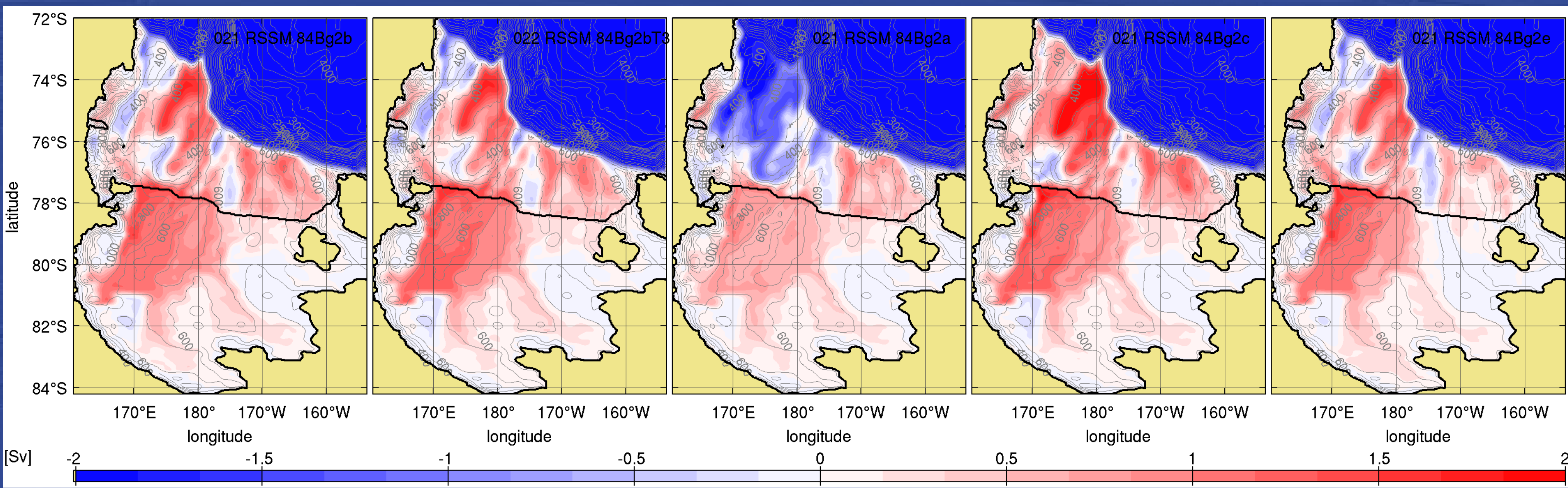

RSSM1 no tides	RSSM2 tides	RSSM1 high wind stress	RSSM1 low wind stress	RSSM1 Hayes Bank experiment
melt -0.14	melt -0.18	melt -0.12	melt -0.16	melt -0.16
freeze 0.01	freeze 0.02	freeze 0.01	freeze 0.01	freeze 0.01

Some Thoughts

➔ realistic model geometry is important! (I think we knew)
➔ the batymetry under the RIS and in the eastern Ross Sea is unclear (?)

➔ melt rates in experiments compared to standard, non-tidal simulation
+18% tides
+14% experimental change in bathymetry
–11% full NCEP wind field
+8% wind stress reduced by sea ice cover (linear)

➔ difficult to predict impacts through future changes in mode 2 & mode 1 heat inflow (MCDW; HSSW)

Some Thoughts

- ➔ realistic model geometry is important! (I think we knew)
- ➔ the batymetry under the RIS and in the eastern Ross Sea is unclear (?)

- ➔ melt rates in experiments compared to standard, non-tidal simulation
  - +18% tides
  - +14% experimental change in bathymetry
  - –11% full NCEP wind field
  - +8% wind stress reduced by sea ice cover (linear)

- ➔ difficult to predict impacts through future changes in mode 2 & mode 1 heat inflow (MCDW; HSSW)

THANK YOU

Appendix

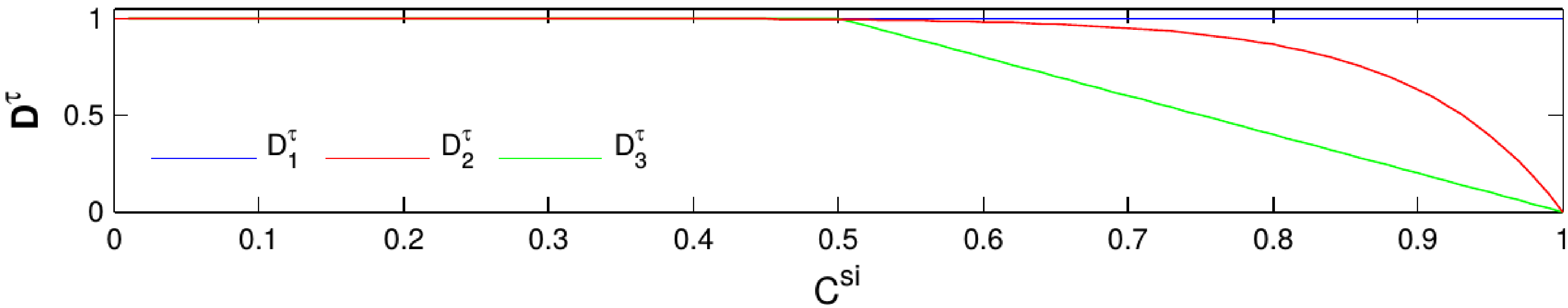

Wind Stress Scenario	Dissipation	Rotation
w1	$\mathcal{D}^\tau_1 = 1$	$\mathcal{R}^\tau(\alpha)$
w2	$\mathcal{D}^\tau_2 = 1 - \mathrm{e}^{\left(\frac{1}{10}C^{si} - 10\right)}$	$\mathcal{R}^\tau(\alpha)$
w3	$\mathcal{D}^\tau_3 = \begin{cases} 1 & \text{for} \quad C^{si} < 50 \\ 2 - \frac{1}{50}C^{si} & \text{for} \quad C^{si} \geq 50 \end{cases}$	$\mathcal{R}^\tau(\alpha)$

$$\mathcal{R}^\tau_{i,j} = \begin{pmatrix} \cos(\alpha_{i,j}) & \sin(\alpha_{i,j}) \\ \text{-}\sin(\alpha_{i,j}) & \cos(\alpha_{i,j}) \end{pmatrix}$$

$$\alpha_{i,j} = 0^\circ(1 - C^{si}_{i,j}) + -25^\circ C^{si}_{i,j}$$

$$\boldsymbol{\tau}' = \mathcal{D}^\tau(C^{si})\boldsymbol{\tau}$$

$$\boldsymbol{\tau}^{si} = \mathcal{R}^\tau(\alpha)\boldsymbol{\tau}'$$

Appendix

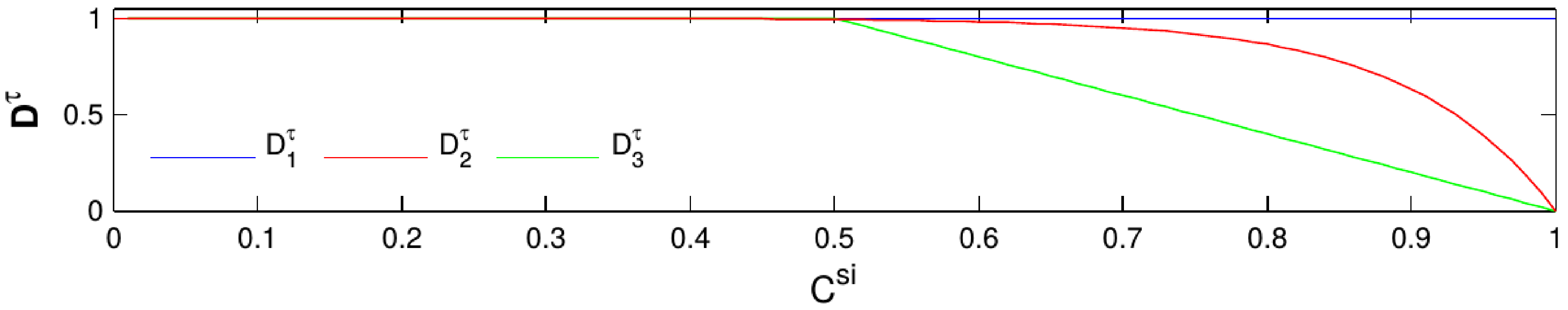

$$\boldsymbol{\tau}^{si} = \mathcal{R}^\tau(\alpha)\boldsymbol{\tau}' \quad \boldsymbol{\tau}' = \mathcal{D}^\tau(C^{si})\boldsymbol{\tau}$$

Wind Stress Scenario	Dissipation	Rotation
w1	$\mathcal{D}_1^\tau = 1$	$\mathcal{R}^\tau(\alpha)$
w2	$\mathcal{D}_2^\tau = 1 - \mathrm{e}^{\left(\frac{1}{10}C^{si} - 10\right)}$	$\mathcal{R}^\tau(\alpha)$
w3	$\mathcal{D}_3^\tau = \begin{cases} 1 & \text{for } C^{si} < 50 \\ 2 - \frac{1}{50}C^{si} & \text{for } C^{si} \geq 50 \end{cases}$	$\mathcal{R}^\tau(\alpha)$

$$\mathcal{R}_{i,j}^\tau = \begin{pmatrix} \cos(\alpha_{i,j}) & \sin(\alpha_{i,j}) \\ -\sin(\alpha_{i,j}) & \cos(\alpha_{i,j}) \end{pmatrix}$$

$$\alpha_{i,j} = 0^\circ(1 - C_{i,j}^{si}) + -25^\circ C_{i,j}^{si}$$

References

Chapman, D. C. (1998). Setting the Scales of the Ocean Response to Isolated Convection*. Journal of Physical Oceanography, 28(4), 606–620.
Årthun, M., Holland, P. R., Nicholls, K. W., & Feltham, D. L. (2013). Eddy-Driven Exchange between the Open Ocean and a Sub–Ice Shelf Cavity. Journal of Physical Oceanography, 43(11), 2372–2387.
Chapman, D. C. (1999). Dense Water Formation beneath a Time-Dependent Coastal Polynya*. Journal of Physical Oceanography, 29(4), 807–820.
Gawarkiewicz, G., & Chapman, D. C. (1995). A numerical study of dense water formation and transport on a shallow, sloping continental shelf. Journal of Geophysical Research, 100(C3), 4489.
Visbeck, M., Marshall, J., & Jones, H. (1997). Dynamics of isolated convective regions in the ocean. M. Visbeck, J. Marshall, H. Jones. 1997. Dynamics of Isolated Convective Regions in the Ocean. Oceanographic Literature Review 44 (6): 542., 6(44), 542.
Wilchinsky, A. V., & Feltham, D. L. (2008). Generation of a Buoyancy-Driven Coastal Current by an Antarctic Polynya. Journal of Physical Oceanography, 38(5), 1011–1032.

Arrigo, K. R. (2003). Phytoplankton dynamics within 37 Antarctic coastal polynya systems. Journal of Geophysical Research, 108(C8), 3271.
Årthun, M., Holland, P. R., Nicholls, K. W., & Feltham, D. L. (2013). Eddy-Driven Exchange between the Open Ocean and a Sub–Ice Shelf Cavity. Journal of Physical Oceanography, 43(11), 2372–2387.

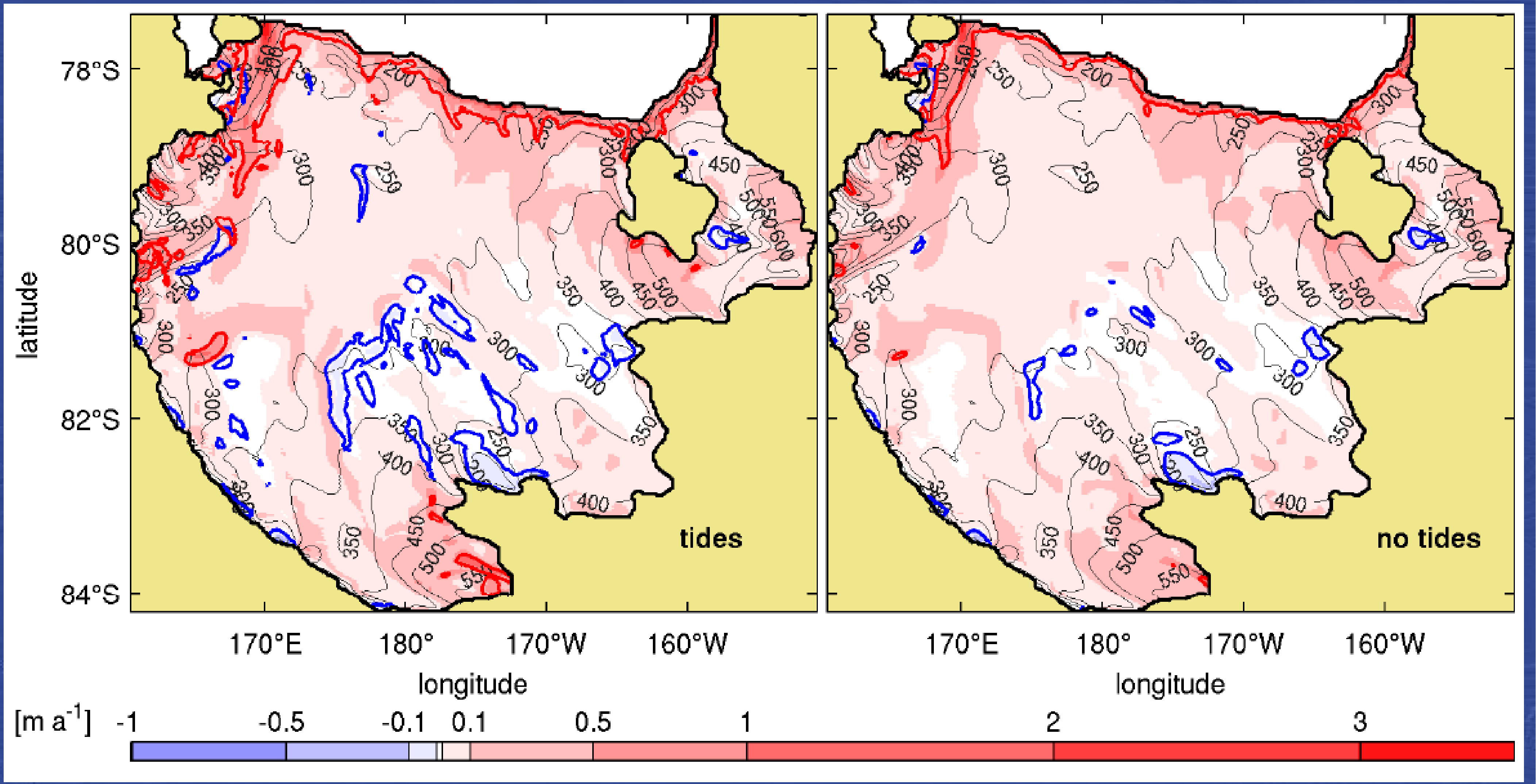

Heat transport also show
And compare to Robin and Mackinson for other ice shelves

Cell C6 - Verfication

Observation

seasonally reversing currents have been observed near the ice shelf edge (Craig Stewart) and on the eastern side of McMurdo Sound (Leonard *et al.*, 2006; Mahoney *et al.*, 2011)

Analytical

$$\Delta\zeta = h\left[\frac{\rho_0 + \sigma_1}{\rho_0 + \sigma_2}\right] \qquad \Delta\zeta = 12\,cm$$

$$h = 500\,m \quad \sigma_1 = 28\,kg\,m^{-3} \quad \sigma_1 = 27.75\,kg\,m^{-3}$$

Other Studies

Gawarkiewicz, G., & Chapman, D. C. (1995);
Visbeck, M., Marshall, J., & Jones, H. (1997);
Chapman, D. C. (1998, 1999);
Wilchinsky, A. V., & Feltham, D. L. (2008);
Årthun, M., Holland,P. R., Nicholls, K. W., & Feltham, D. L. (2013)

Aspects of Circulation in the Ross Sea

- ➔ horizontal circulation structure
- ➔ transport volumes
- ➔ annual transport variation
- ➔ depth structure of dynamics
- ➔ **driving mechanisms**
- ➔ what water types
- ➔ origin and destination of water bodies

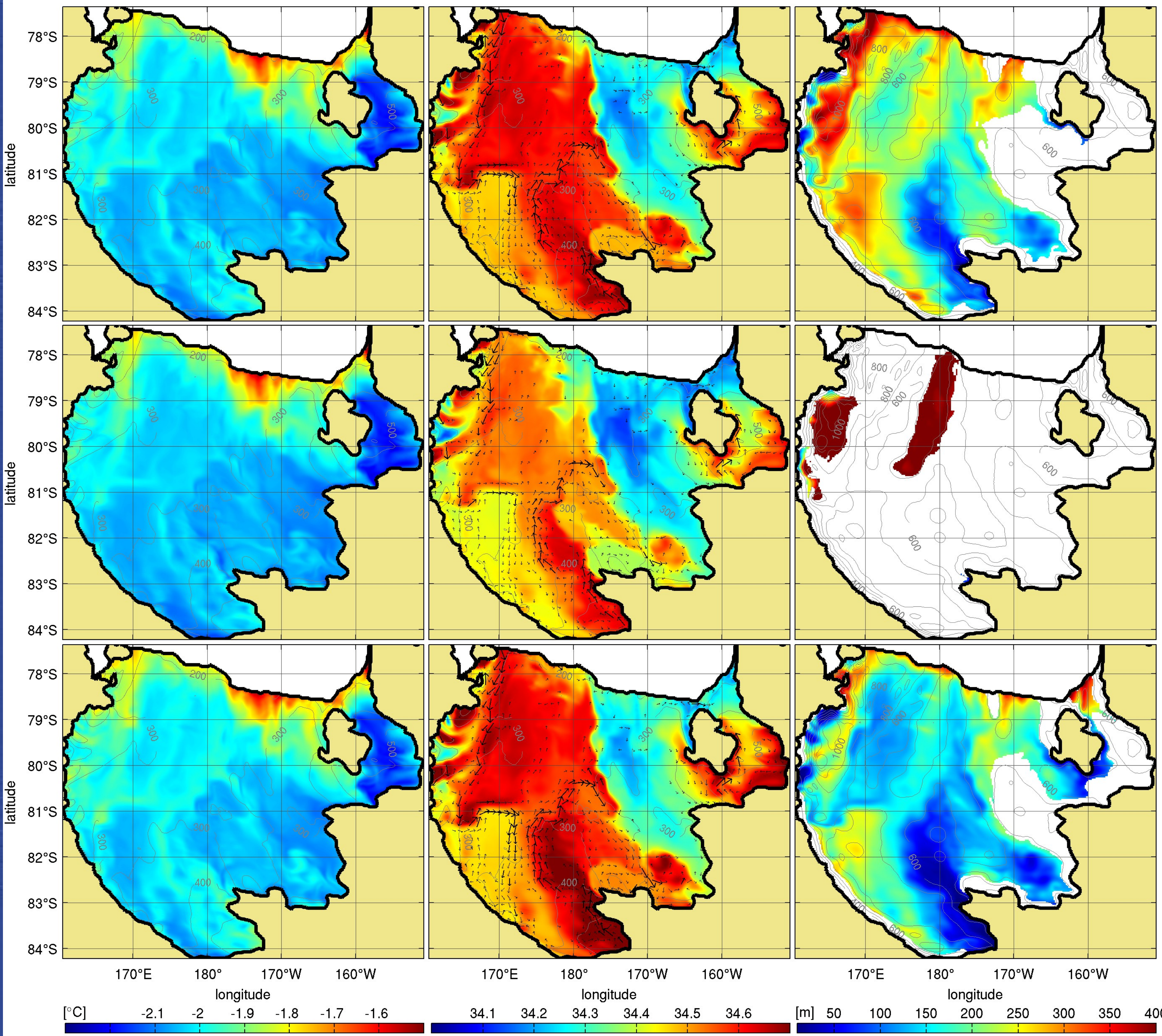
78°S
79°S
80°S
81°S
82°S
83°S
84°S
latitude
170°E
180°
170°W
160°W
longitude
[°C]
-2.1
-2
-1.9
-1.8
-1.7
-1.6
34.1
34.2
34.3
34.4
34.5
34.6
[m]
50
100
150
200
250
300
350
400

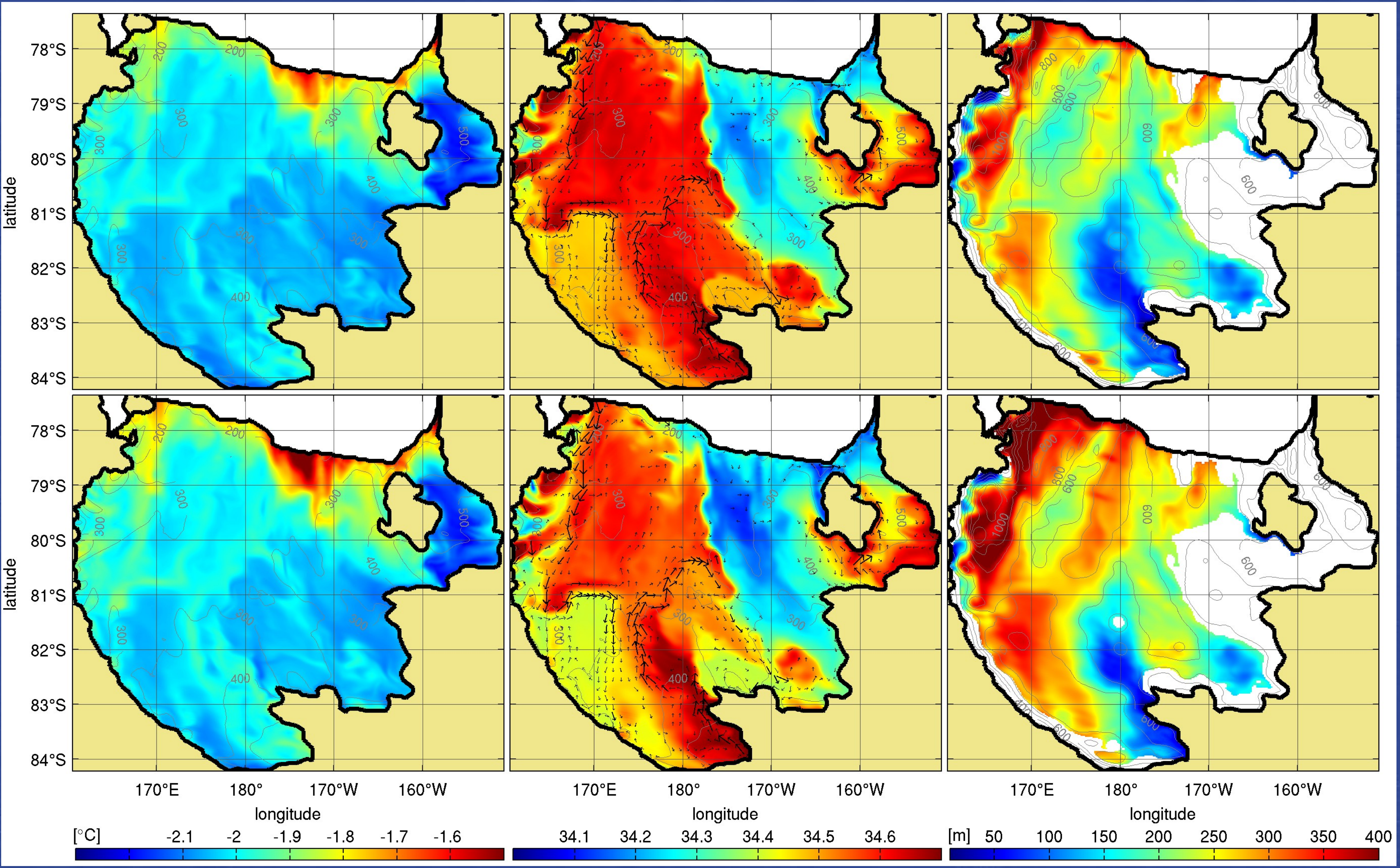

78°S
79°S
80°S
81°S
82°S
83°S
84°S
latitude
170°E
180°
170°W
160°W
longitude
[°C] -2.1 -2 -1.9 -1.8 -1.7 -1.6
34.1 34.2 34.3 34.4 34.5 34.6
[m] 50 100 150 200 250 300 350 400

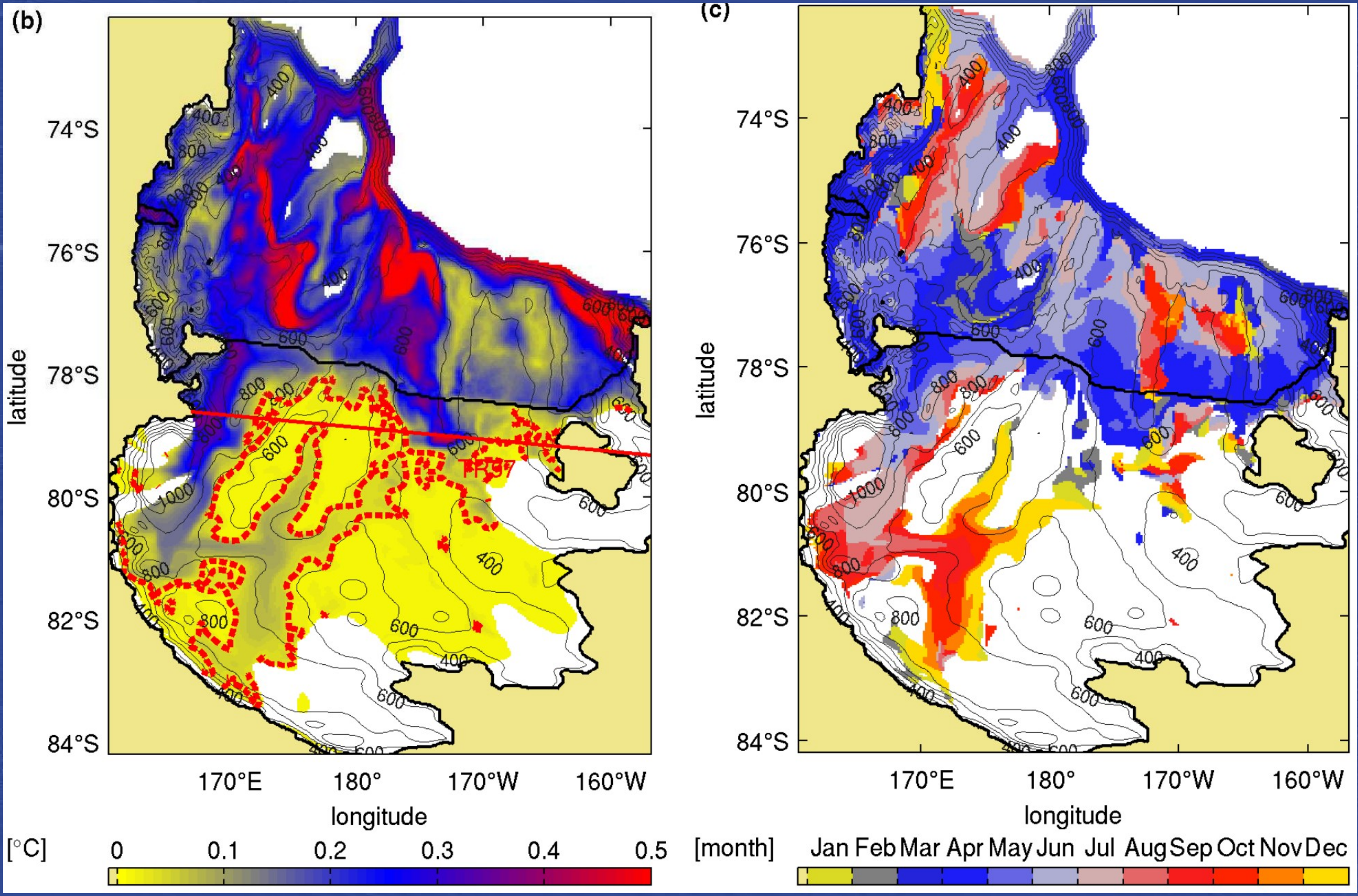

Desynced SW and CDW heat signals

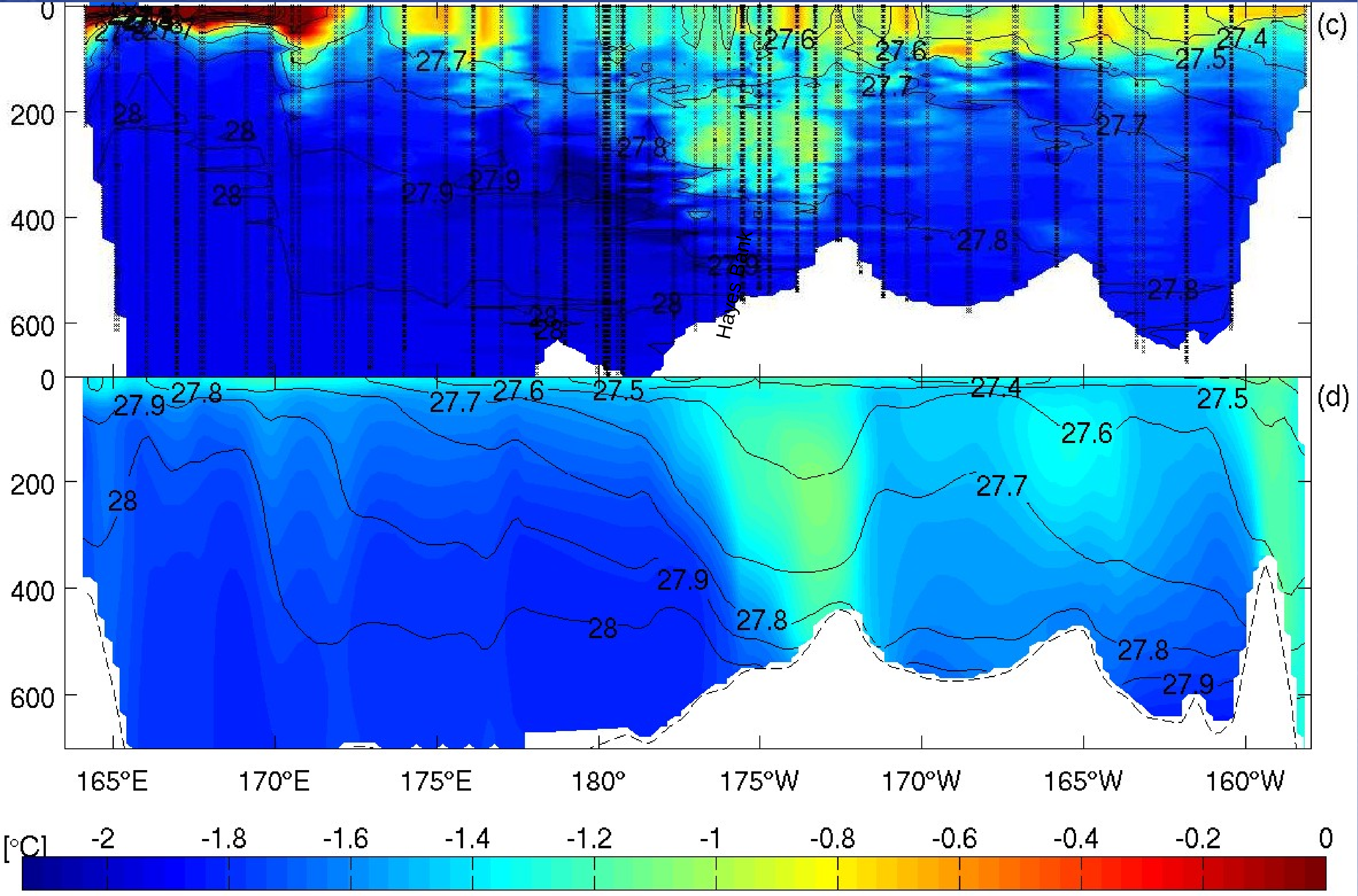

(c)
(d)
27.4
27.5
27.6
27.7
27.8
27.9
28
Hayes Bank
0
200
400
600
165°E
170°E
175°E
180°
175°W
170°W
165°W
160°W
[°C]
-2
-1.8
-1.6
-1.4
-1.2
-1
-0.8
-0.6
-0.4
-0.2
0

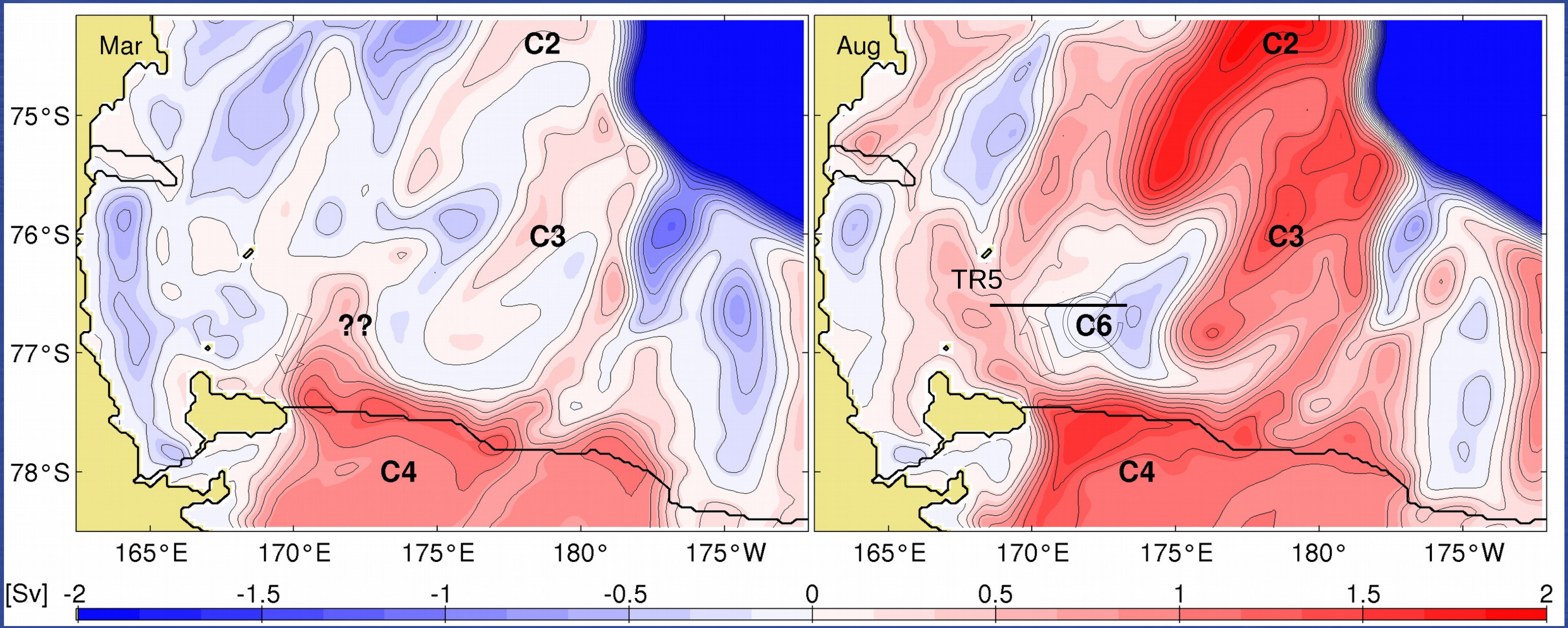

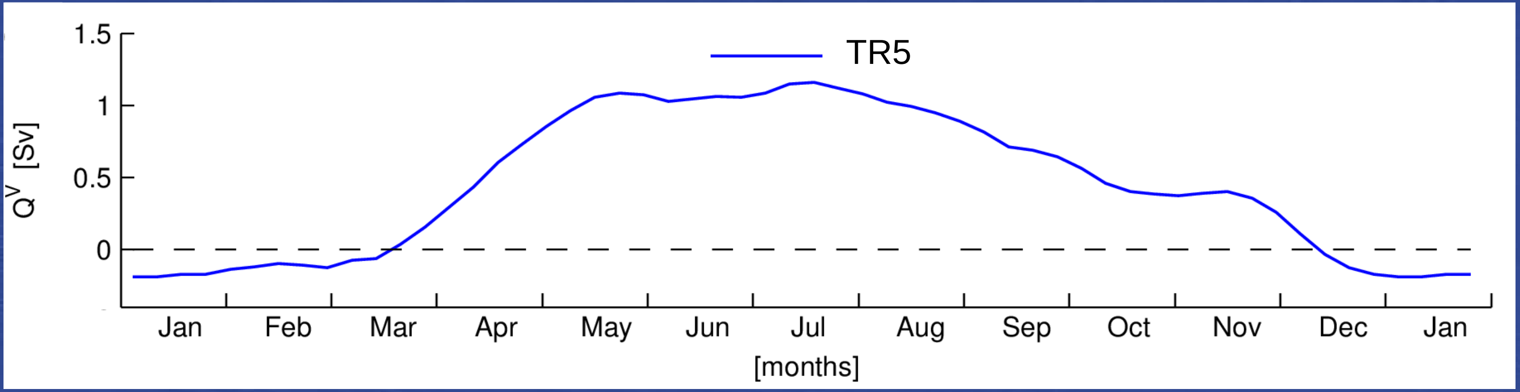

➔ seasonally reversing current creates *RSP eddy* in April-November

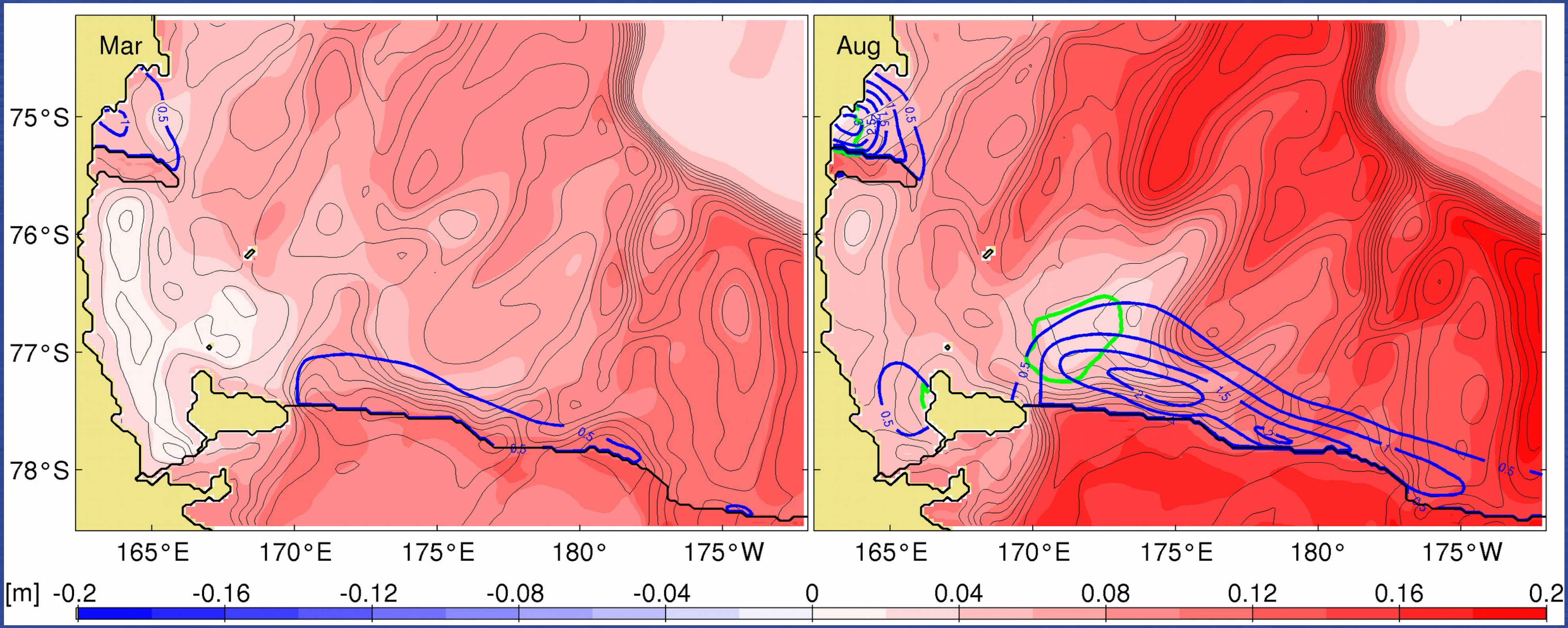

- ➔ brine ejection from sea ice production in the RSP
- ➔ deep convection chimney forms
- ➔ SSH depression from thermostatic contraction of the water column
- ➔ strong lateral SSH gradient exerts barotropic pressure gradient
- ➔ resulting geostrophic transports can reverse the baroclinic flows

The Victoria Land Coastal Current

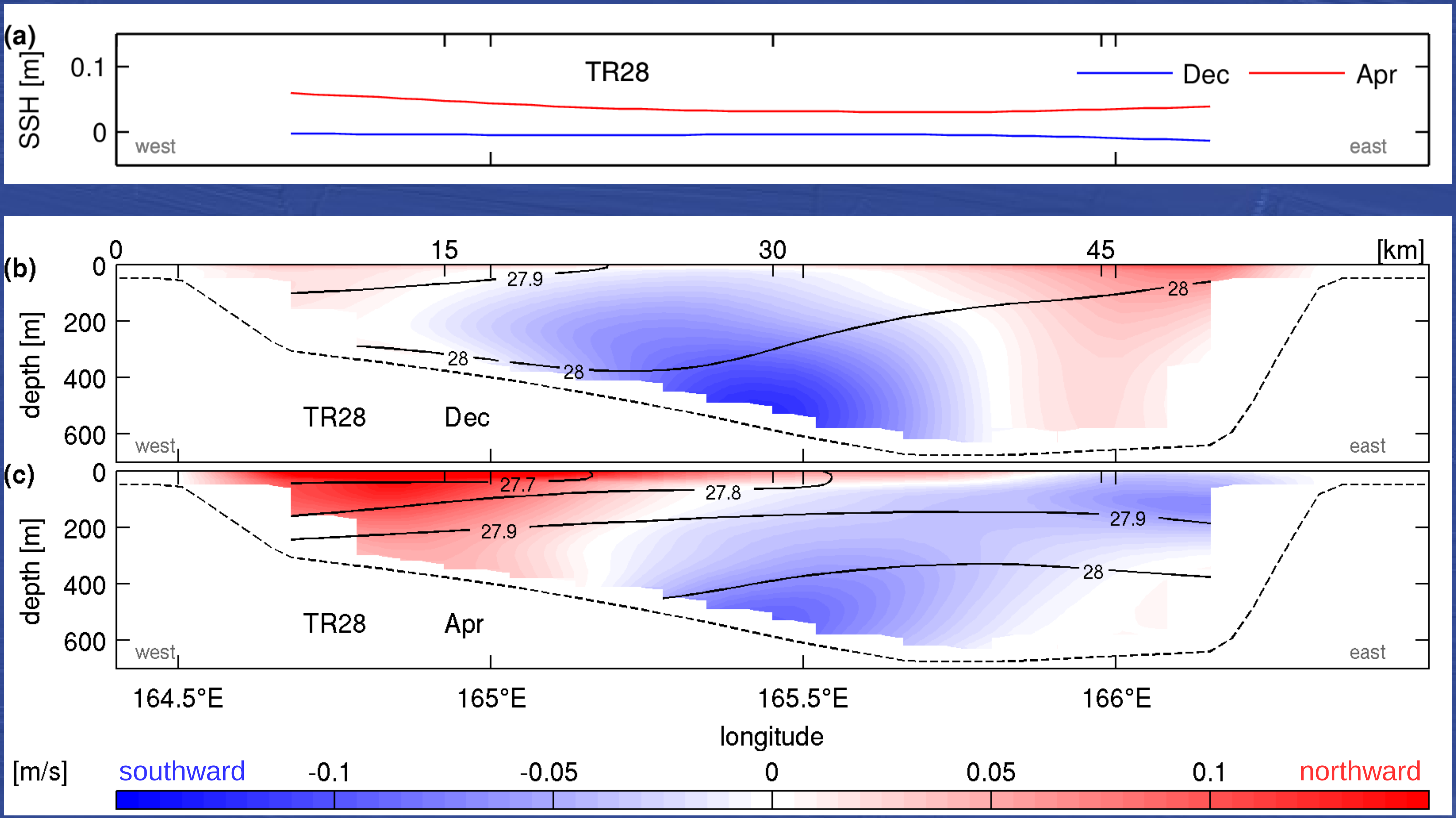

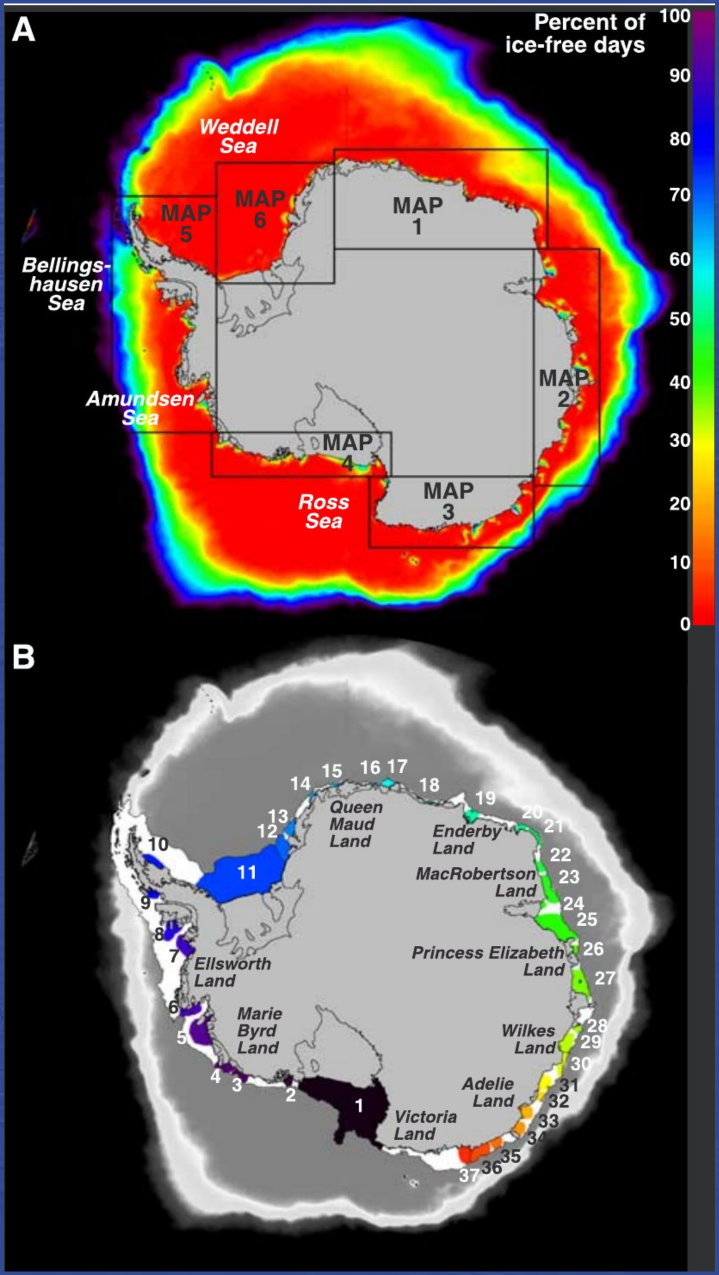

Arrigo (2003)

Barber & Masson (2007)

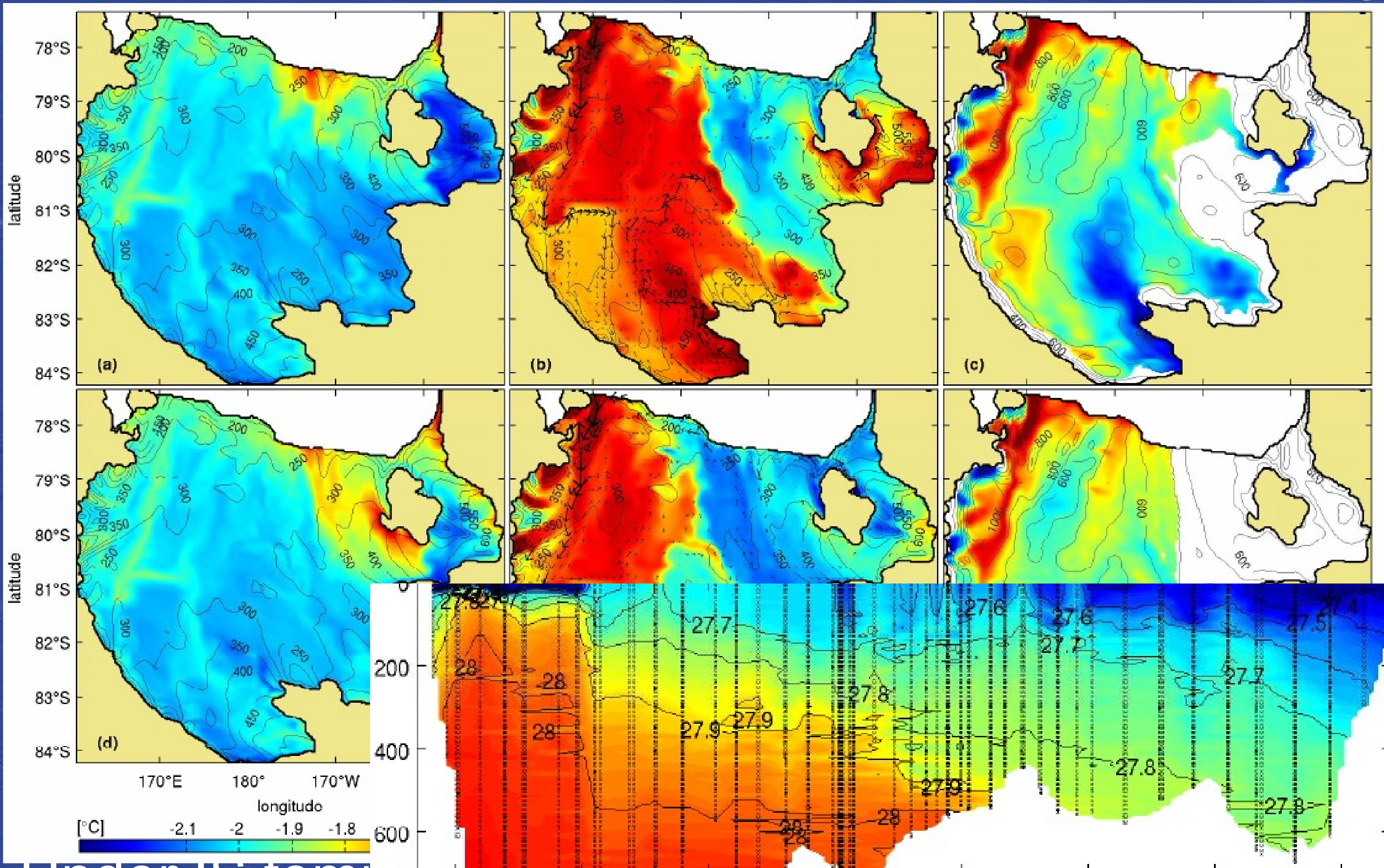

Under IS temp & salt wind, tides and bathy

Circulation Cell 6